NFN - Nationales Forschungsnetzwerk

Geometry + Simulation

http://www.gs.jku.at

Decoupled Patchwork B-splines

Nora Engleitner, Bert Jüttler,

G+S Report No. 81

April 2019

Der Wissenschaftsfonds.

JOHANNES KEPLER UNIVERSITY LINZ

Decoupled Patchwork B-splines

Nora Engleitner, Bert Jüttler

Institute of Applied Geometry, Johannes Kepler University, Linz

Abstract

We consider hierarchies that consist of a partition of the d-dimensional unit cube into patches and an associated tensor-product spline space for each of them. The spline spaces possess uniform degree $\mathbf{p}$ and maximum smoothness $C^{\mathbf{p}-\mathbf{1}}$, but potentially different knots. Under certain assumptions on this hierarchy, we show how to construct Decoupled Patchwork B-splines (DPB-splines) that span the corresponding patchwork spline space $\mathbb{P}$. More precisely, we generate a basis for the space $\mathbb{P}$ formed by all $C^{\mathbf{p}-\mathbf{1}}$ smooth functions that admit patch-wise representations in the associated spline spaces. Based on the framework of decoupled tensor-product B-splines [1], we obtain a basis that is algebraically complete, forms a convex partition of unity and preserves the coefficients of the local B-spline representations. Furthermore, we present an adaptive refinement algorithm for surface approximation that generates hierarchies, which satisfy the required assumptions and hence can be equipped with a DPB-spline basis.

Keywords: adaptive refinement, anisotropic refinement, hierarchical splines, algebraic completeness, surface approximation

1. Introduction

Tensor-product B-splines, which are the standard for describing free-form geometries in Computer-Aided Design, e.g., see [2], possess a fundamental limitation: Their tensor-product structure does not support local refinement. Therefore, adaptive spline constructions have been developed in order to overcome this restriction and provide more flexibility in design and analysis. Forsey and Bartels were the first to introduce hierarchical B-spline refinement [3]. Their hierarchical construction was later extendend by Kraft, who developed a selection mechanism that defines a basis for the hierarchical spline space [4].

T-splines [5] have been developed as an adaptive construction on meshes with T-joints. In general these splines are not linearly independent and therefore, analysis-suitable (AS) T-splines and AS++ T-splines have been introduced and discussed in [6, 7, 8, 9]. Moreover, polynomial splines over hierarchical T-meshes [10, 11] and locally refined B-splines [12] have been established. Recently, the latter construction has been generalized to LR T-splines [13], where local refinement is performed on an initial T-mesh instead of a tensor-product mesh.

In order to restore the partition of unity property for hierarchical splines, a truncation mechanism has been introduced in [14]. The resulting truncated hierarchical B-splines

(THB-splines) possess good mathematical properties, see [15, 16, 17] for a detailed analysis of stability, completeness and approximation power. Applications of (T)HB-splines include surface approximation [18, 19, 20] and isogeometric analysis [21, 22, 23, 24, 25, 26]. Aspects of the implementation have been discussed in [27, 28]. Moreover, the hierarchical principle has been applied to other constructions, such as Powell-Sabin splines [29], triangular splines [30], box splines [31, 32, 33], B-splines on triangulations [34], T-splines [35, 36], and subdivision spline functions [37, 38].

While THB-splines have good mathematical properties, they are not as flexible as other constructions like T-splines or LR B-splines. To be more precise, hierarchical B-splines rely on a sequence of nested spline spaces and therefore, the choice of possible refinement strategies is limited. Recently, we generalized hierarchical splines to Patchwork B-splines (PB-splines), which are defined on a sequence of partially nested spline spaces and enable the use of independent refinement strategies in different parts of the domain [39, 40]. An adapted version of Kraft's selection mechanism constructs a basis for the patchwork spline space under certain assumptions. Similar to the hierarchical splines, a truncation mechanism has been established in order to obtain a basis of truncated PB-splines (TPB-splines) that forms a non-negative partition of unity. Applications of the PB-splines in surface approximation and to lofting B-spline curves [41] have shown the potential of this new construction.

Although the (T)PB-splines provide increased flexibility, there are still certain limitations on the available refinement strategies. For instance, a region that separates two coarser spline spaces is required to have a certain degree-dependent width, see Fig. 1. Additionally, the spaces that are present in a degree-dependent neighborhood of any cell need to be (upwards or downwards) compatible with the chosen space for this cell if TPB-splines are to be generated. Consequently, a region that separates two finer (but non-nested) refinement regions is also required to possess a certain degree-dependent width, see Fig. 2. For instance, also the PB-spline hierarchies considered in [41] for solving the lofting problem do not admit TPB-splines.

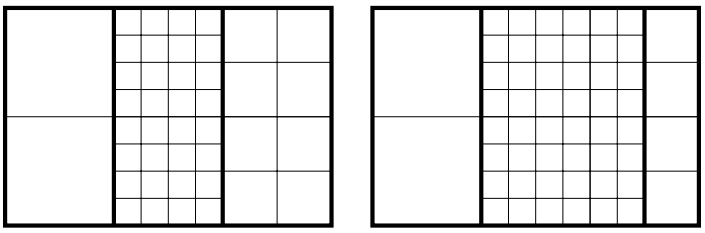

Figure 1: Invalid (left) and valid (right) meshes for bicubic (T)PB-splines.

Finally we note that (T)PB-splines are not algebraically complete in general. This is similar to THB-splines, see [1], where the use of decoupled B-splines led to significant improvements. We build on this idea to define the new framework of *Decoupled Patchwork B-splines* (DPB-splines). More precisely, we define local basis functions, called patch B-splines, that are obtained by restricting and decoupling tensor-product B-splines.

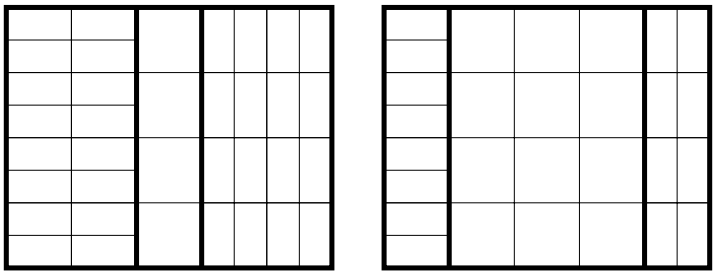

Figure 2: Invalid (left) and valid (right) meshes for bicubic TPB-splines.

The remainder of this paper is organized as follows: Chapter 2 introduces the general framework consisting of patches, the local spline spaces and a patchwork spline space. A truncation and selection mechanism are then used to define the DPB-splines. In Chapter 3 we identify assumptions that are needed in order to guarantee a certain order of smoothness of the basis functions and for characterizing the obtained spline space. These assumptions affect only a patch and its neighbors. The mathematical properties of the DPB-splines are analyzed in Chapter 4. In particular, the basis functions possess continuous values and derivatives up to a certain order, they span the patchwork spline space and form a convex partition of unity. Moreover, we observe that the patchwork spline space is equal to the full spline space, i.e., the basis is algebraically complete. In Chapter 5 we identify a simple sufficient condition for a certain class of patches that guarantees that the assumptions are satisfied. Finally, we provide an improved refinement algorithm for least-squares fitting in Chapter 6, which generates hierachies that can be equipped with a Decoupled Patchwork and a (truncated) Patchwork B-spline basis. Two examples are used to illustrate the advantages of this new strategy. Finally, we conclude the paper in Chapter 7.

2. The general framework

For defining Decoupled Patchwork B-splines we construct a hierarchy consisting of patches and corresponding spaces, which are not necessarily nested. The basis functions are then obtained by applying a truncation and selection mechanism to local bases. Furthermore, we introduce a spline space, which is defined on the hierarchy.

2.1. Patches

We consider a finite sequence of *patches* $\{\pi^\ell\}_{\ell=1,\dots,N}$, which are closed subsets of the d–dimensional unit cube $[0,1]^d$. The upper index ℓ will be called the *level*. The patches possess a mutually disjoint interior, $\mathrm{int}(\pi^\ell) \cap \mathrm{int}(\pi^k) = \emptyset$, for $k \neq \ell$, and their union defines the *domain*,

$$\Omega = \bigcup_{\ell=1}^{N} \pi^\ell.$$

Not only the entire domain but certain subsets thereof will be used in the remainder of the paper. An index set $\mathcal{D} \subseteq \{1, \ldots, N\}$ generates the *subdomain*,

$$\Delta_{\mathcal{D}} = \bigcup_{\ell \in \mathcal{D}} \pi^{\ell} \subseteq \Omega. \tag{1}$$

In particular, we define $\Delta_{\mathcal{D},\geq\ell} = \Delta_{\mathcal{D}} \cap \Delta_{\geq\ell}$, with the index set $\geq\ell = \{\ell, \ldots, N\}$, as the subdomain formed by all patches in $\Delta_{\mathcal{D}}$ with level greater or equal to ℓ. Furthermore, we introduce the index set

$$\mathcal{N}^{\ell} = \{k \ : \ k > \ell \text{ and } \pi^k \cap \pi^{\ell} \neq \emptyset\},$$

that comprises the levels $k > \ell$ of higher level neighboring patches of π^{ℓ}. The index set of higher level neighboring patches in $\Delta_{\mathcal{D}}$ will be denoted as

$$\mathcal{N}^{\ell}_{\mathcal{D}} = \mathcal{N}^{\ell} \cap \mathcal{D}.$$

The two index sets $\mathcal{N}^{\ell}$ and $\mathcal{N}^{\ell}_{\mathcal{D}}$ define the subdomains $\Delta_{\mathcal{N}^{\ell}}$ and $\Delta_{\mathcal{N}^{\ell}_{\mathcal{D}}}$, respectively.

Example 1. We consider the subdivision of the unit square into six patches, $\pi^1, \ldots, \pi^6$. Note that the patches might possess several connected components, as it is the case for patch π^2 in this example. Fig. 3 depicts several subdomains of Ω. The subdomain $\Delta_{\geq 3}$ is formed by the patches $\pi^3, \ldots, \pi^6$ as illustrated in Fig. 3a. Consider $\mathcal{D} = \{2, 4, 5\}$, thus $\Delta_{\mathcal{D},\geq 3} = \pi^4 \cup \pi^5$, see Fig. 3b. The higher level neighbors of π^3 define the index set $\mathcal{N}^3 = \{4, 6\}$, see Fig. 3c. The intersection of $\Delta_{\mathcal{N}^3}$ and $\Delta_{\mathcal{D}}$ gives the subdomain $\Delta_{\mathcal{N}^3_{\mathcal{D}}}$, which consists of π^4, see Fig. 3d. ◊

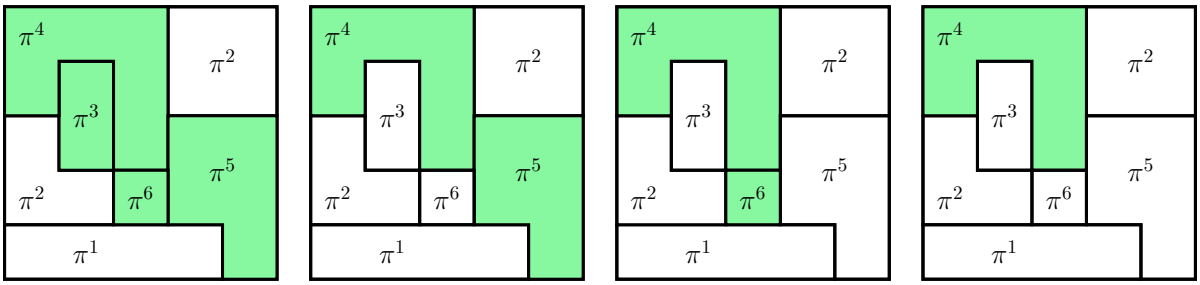

Figure 3: Example 1 – The subdomains $\Delta_{\geq 3}$, $\Delta_{\mathcal{D},\geq 3}$, $\Delta_{\mathcal{N}^3}$ and $\Delta_{\mathcal{N}^3_{\mathcal{D}}}$ (a-d) for $\mathcal{D} = \{2, 4, 5\}$.

Except for trivial situations, each patch shares parts of its boundary $\partial\pi^{\ell}$ with patches of a different level. The part of the boundary that intersects with patches of a *higher* level will be called the *constraining boundary*,

$$\Gamma^{\ell} = \Delta_{\geq\ell+1} \cap \pi^{\ell}.$$

In addition we define the constraining boundary

$$\Gamma^{\ell}_{\mathcal{D}} = \Gamma^{\ell} \cap \Delta_{\mathcal{D}} = \Delta_{\mathcal{D},\geq\ell+1} \cap \pi^{\ell},$$

with respect to the subdomain $\Delta_{\mathcal{D}}$.

Example 1 (continuing from p. 4)**.** Fig. 4 shows the constraining boundaries Γ^4, $\Gamma^4_{\mathcal{D}}$, $\Gamma^4_{\mathcal{N}^3}$ and $\Gamma^4_{\mathcal{N}^3_{\mathcal{D}}} = \emptyset$. ♢

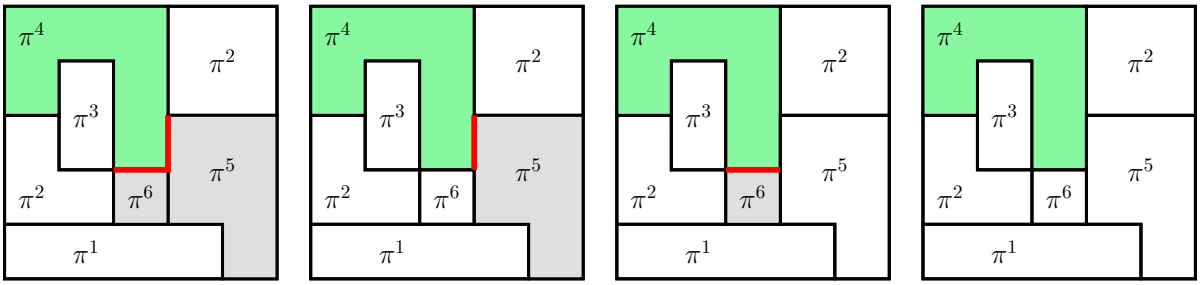

Figure 4: Example 1 – The constraining boundaries Γ^4, $\Gamma^4_{\mathcal{D}}$, $\Gamma^4_{\mathcal{N}^3}$ and $\Gamma^4_{\mathcal{N}^3_{\mathcal{D}}} = \emptyset$ (a-d).

2.2. Spline spaces

For each level ℓ, we choose a globally[1] defined tensor-product spline basis $\hat{B}^\ell$ that consists of individual basis functions $\hat{\beta}^\ell \in \hat{B}^\ell$, spanning a certain spline space $\hat{\mathbb{V}}^\ell$. Note that we consider sets $\hat{B}^\ell$ of basis functions and use the symbol $\hat{\beta}^\ell$ to represent their elements. The upper index indicates the level but does not identify individual basis functions.

More precisely, the basis functions are tensor-product B-splines of degree $\mathbf{p} = (p_1, \dots, p_d)$ defined on d open knot vectors with $(p_i + 1)$-fold boundary knots 0 and 1. All inner knots possess multiplicity 1. Hence, we obtain B-splines of maximal smoothness, $C^{\mathbf{s}}(\Omega)$, with $\mathbf{s} = \mathbf{p} - \mathbf{1}$. In other words, the basis functions possess continuous values and partial derivatives up to order $p_i - 1$ in each variable x_i separately. The supports[2] of the functions $\hat{\beta}^\ell$ are axis-aligned open boxes in $[0, 1]^d$.

In addition to the B-spline bases, which are independent of the patches π^ℓ, we define *local* spline bases B^ℓ on π^ℓ that consist of *patch B-splines* β^ℓ and span the spaces $\mathbb{V}^\ell$. The basis functions are constructed by *decoupling* the restricted function $\hat{\beta}^\ell|_{\pi^\ell}$, see [1]. More precisely, for each connected component φ of $\mathrm{supp}\hat{\beta}^\ell \cap \pi^\ell$ we obtain a basis function

$$\beta^\ell = \begin{cases} \hat{\beta}^\ell & \text{on } \varphi \\ 0 & \pi^\ell \setminus \varphi. \end{cases} \tag{2}$$

Example 2. We consider three different biquadratic tensor-product B-splines $\hat{\beta}^\ell$ and discuss the resulting patch B-splines with respect to a U-shaped patch π^ℓ, represented as gray area in Fig. 5. The knot vectors of level ℓ define the grid that is illustrated in the three pictures. The supports the B-splines are depicted as blue squares, and the blue circles

[1] i.e., with domain $[0, 1]^d$

[2] Note that we use the set-theoretic definition of the support, i.e., for a function $f : \Omega \mapsto \mathbb{R}^d$ the support of f is defined as $\mathrm{supp} f = \{\mathbf{x} \in \Omega \ : \ f(\mathbf{x}) \neq 0\}$.

indicate their Greville points. Depending on the location of the support with respect to the patch we obtain zero, one or two patch B-splines. ◊

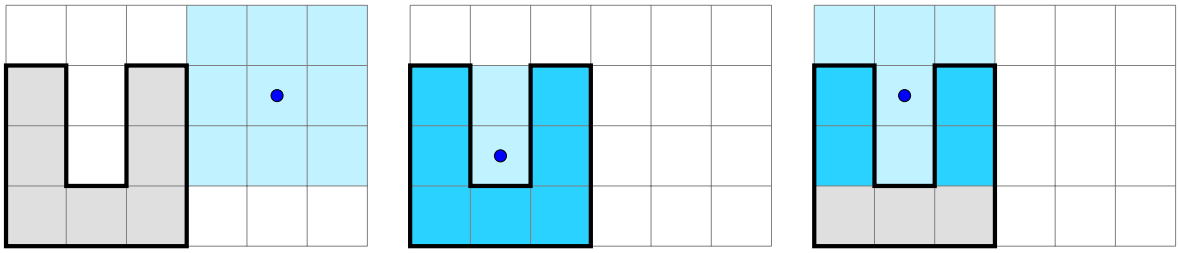

(a) (b) (c)

Figure 5: Example 2 – Restriction of three tensor-product B-splines to a U-shaped patch.

The functions in B^ℓ possess good mathematical properties on π^ℓ: They are linearly independent, non-negative, form a partition of unity and have continuous values and partial derivatives up to order $p_i - 1$ in each variable x_i. The dual functionals, which generate the coefficients of the local representation

$$f(\mathbf{x}) = \sum_{\beta^\ell \in B^\ell} \lambda_{\beta^\ell}(f)\beta^\ell(\mathbf{x}), \quad \text{for } \mathbf{x} \in \pi^\ell,$$

of a function $f \in \mathbb{V}^\ell$, will be denoted by $\lambda_{\beta^\ell}(.)$.

For later reference we note that

$$\text{supp}\beta^k \cap \Gamma^\ell = \text{supp}\beta^k \cap \Gamma^\ell_{\mathcal{D}}, \tag{3}$$

for $\beta^k \in B^k$ and any index set $\mathcal{D}$ with $k \in \mathcal{D}$ and $\ell < k$.

We introduce the *extension operator*, $\mathcal{E} : B^\ell \mapsto \hat{B}^\ell$, that transforms a patch B-spline $\beta^\ell \in B^\ell$ into the globally defined tensor-product B-spline $\mathcal{E}(\beta^\ell) = \hat{\beta}^\ell \in \hat{B}^\ell$ such that

$$\beta^\ell = \hat{\beta}^\ell|_{\text{supp}\beta^\ell}. \tag{4}$$

The extension of a patch B-spline β^ℓ is always denoted by $\hat{\beta}^\ell$ in the remainder of this paper. Note that different patch B-splines β^ℓ and β'^ℓ with disjoint supports possess the same extension $\hat{\beta}^\ell = \hat{\beta}'^\ell$ if they are derived from the same tensor-product B-spline. It follows that $\hat{\beta}^\ell|_{\pi^\ell} \in \mathbb{V}^\ell$ since

$$\hat{\beta}^\ell|_{\pi^\ell} = \sum_{\substack{\beta'^\ell \in B^\ell \\ \hat{\beta}'^\ell = \hat{\beta}^\ell}} \beta'^\ell.$$

Furthermore, if the spaces spanned by a pair of spline bases $\hat{B}^\ell$ and $\hat{B}^k$ are nested, i.e., $\hat{\mathbb{V}}^\ell \subseteq \hat{\mathbb{V}}^k$, for $\ell < k$, then it holds that $\hat{\beta}^\ell|_{\pi^k} \in \mathbb{V}^k$ and

$$\lambda_{\beta^k}(\hat{\beta}^\ell) = \lambda_{\hat{\beta}^k}(\hat{\beta}^\ell), \tag{5}$$

where the values $\lambda_{\hat{\beta}^k}(\hat{\beta}^\ell)$ of the dual functionals are the coefficients obtained by B-spline refinement.

We conclude this subsection by introducing the *patchwork spline space*. On a general subdomain $\Delta_{\mathcal{D}}$ we define,

$$\mathbb{P}_{\mathcal{D}} = \{f \in C^{\mathbf{s}}(\Delta_{\mathcal{D}}) \ : \ f|_{\pi^k} \in \mathbb{V}^k, \text{ for } k \in \mathcal{D}\}.$$

Note that the tensor-product polynomials of degree $\mathbf{p}$ restricted to the subdomain $\Delta_{\mathcal{D}}$ are contained in the patchwork spline space $\mathbb{P}_{\mathcal{D}}$. With $\mathbb{P}_{\mathcal{D},\geq\ell}$ we denote the the patchwork spline space on the subdomain $\Delta_{\mathcal{D},\geq\ell}$, while $\mathbb{P} = \mathbb{P}_{\geq 1}$ is the patchwork spline space on the entire domain.

2.3. Basis

Our construction is based on the natural assumption that the spline spaces associated with neighboring patches are nested.

Assumption 1 (Nested Neighbor Condition – NNC)**.** *Any two globally defined spline spaces satisfy* $\hat{\mathbb{V}}^\ell \subseteq \hat{\mathbb{V}}^k$ *if* $k \in \mathcal{N}^\ell$.

We construct a basis by adapting Kraft's selection mechanism [4] to the patch structure. The *Decoupled Patchwork B-splines* $P_{\mathcal{D}}$ on the subdomain $\Delta_{\mathcal{D}}$ are computed recursively, starting at the highest level N and using the initialization $P_{\mathcal{D}}^{N+1} = \emptyset$. Since the index set $\mathcal{D}$ does not necessarily contain all levels, we distinguish between two cases: When proceeding to the next lower level ℓ, the DPB-splines remain unchanged if $\ell \notin \mathcal{D}$. Otherwise, they are defined as the union of *selected* and *truncated* patch B-splines,

$$P_{\mathcal{D}}^\ell = \begin{cases} S_{\mathcal{D}}^{\ell+1} \cup T_{\mathcal{D}}^\ell & \text{if } \ell \in \mathcal{D} \\ P_{\mathcal{D}}^{\ell+1} & \text{otherwise.} \end{cases}$$

More precisely, we *select* functions of levels higher than ℓ that vanish on the constraining boundary,

$$S_{\mathcal{D}}^{\ell+1} = \{\tilde{\beta}_{\mathcal{D}}^k \in P_{\mathcal{D}}^{\ell+1} \ : \ \tilde{\beta}_{\mathcal{D}}^k = 0 \quad \text{on} \quad \Gamma_{\mathcal{D}}^\ell\},$$

and apply *truncation* – indicated by the tilde operator – to the extensions of the patch B-splines of level ℓ,

$$T_{\mathcal{D}}^\ell = \{\tilde{\beta}_{\mathcal{D}}^\ell \ : \ \beta^\ell \in B^\ell\}.$$

More precisely, the *truncated patch B-splines* $\tilde{\beta}_{\mathcal{D}}^\ell$, for $\ell \in \mathcal{D}$, are equal to the patch B-splines on π^ℓ and extend smoothly (as we shall see later) into $\Delta_{\mathcal{D},\geq\ell} \setminus \pi^\ell$,

$$\tilde{\beta}_{\mathcal{D}}^\ell = \begin{cases} \beta^\ell & \text{on } \pi^\ell \\ \displaystyle\sum_{\substack{\tilde{\beta}_{\mathcal{D}}^k \in P_{\mathcal{D}}^{\ell+1} \\ \operatorname{supp}\beta^\ell \cap \operatorname{supp}\beta^k \neq \emptyset}} \lambda_{\beta^k}(\hat{\beta}^\ell)\, \tilde{\beta}_{\mathcal{D}}^k & \text{on } \Delta_{\mathcal{D},\geq\ell} \setminus \pi^\ell \\ 0 & \text{elsewhere.} \end{cases} \tag{6}$$

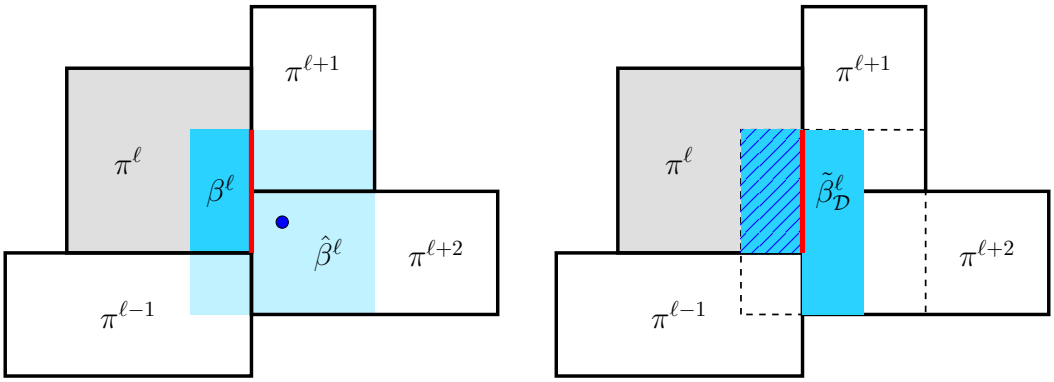

Figure 6: The supports of a patch B-spline β^ℓ (blue) and its extension $\hat{\beta}^\ell$ (light blue) are shown in (a). The corresponding truncated patch B-spline $\tilde{\beta}^\ell_{\mathcal{D}}$ is illustrated in (b). In the hatched area the truncated patch B-spline is equal to the patch B-spline and the non-hatched part represents the smooth extension to $\Delta_{\mathcal{D},\geq\ell} \setminus \pi^\ell$.

The support condition $\text{supp}\beta^\ell \cap \text{supp}\beta^k \neq \emptyset$ implies that the truncated functions are linear combinations of non-selected basis functions of higher levels on $\Delta_{\mathcal{D},\geq\ell} \setminus \pi^\ell$, i.e., of basis functions that do not vanish on the constraining boundary $\Gamma^\ell_{\mathcal{D}}$, see Fig. 6. Note that the sum in (6) considers only basis functions of patches π^k, with $k > \ell$, that are neighbors of π^ℓ, i.e., $k \in \mathcal{N}^\ell \cap \mathcal{D}$. According to NNC it follows that $\hat{\beta}^\ell|_{\pi^k} \in \mathbb{V}^k$ and therefore, the coefficients $\lambda_{\beta^k}(\hat{\beta}^\ell)$ exist and are non-negative due to the properties of B-spline refinement, see Eq. (6).

After completing the recursion we obtain $P_{\mathcal{D}} = P^1_{\mathcal{D}}$ and $P = P_{\geq 1}$.

Lemma 1. *The truncated patch B-splines $\tilde{\beta}^k_{\mathcal{D}} \in T^k_{\mathcal{D}}$ satisfy*

$$\text{supp}\tilde{\beta}^k_{\mathcal{D}} \subseteq \text{supp}\hat{\beta}^k. \tag{7}$$

Proof. We prove this statement by induction starting from level $n = \max\{k \in \mathcal{D}\}$, which is decreased until we arrive at $n = 1$. According to the piecewise definition of $\tilde{\beta}^n_{\mathcal{D}}$ it follows immediately that

$$\text{supp}\tilde{\beta}^n_{\mathcal{D}} = \text{supp}\beta^n \subseteq \text{supp}\hat{\beta}^n.$$

Now we assume that (7) is satisfied for $k \geq \bar{k} \in \mathcal{D}$ and it remains to be shown that the statement holds as well for $\ell = \max\{m \in \mathcal{D} \ : \ m < \bar{k}\}$. We consider a basis function $\tilde{\beta}^\ell_{\mathcal{D}} \in T^\ell_{\mathcal{D}}$. Note that

$$\{\tilde{\beta}^k_{\mathcal{D}} \in P^{\ell+1}_{\mathcal{D}} \ : \ \text{supp}\beta^k \cap \text{supp}\beta^\ell \neq \emptyset\} \subseteq \{\tilde{\beta}^k_{\mathcal{D}} \in T^k_{\mathcal{D}} \ : \ \ell < k \in \mathcal{D} \ \wedge \ \text{supp}\beta^k \cap \text{supp}\beta^\ell \neq \emptyset\}.$$

Thus, it follows from the definition of $\tilde{\beta}^\ell_{\mathcal{D}}$ and the induction hypothesis that

$$\text{supp}\tilde{\beta}^\ell_{\mathcal{D}} \subseteq \text{supp}\beta^\ell \cup \Big(\bigcup_{k\in\mathcal{D},\, k>\ell} \ \bigcup_{\substack{\beta^k \in B^k \\ \text{supp}\beta^k \cap \text{supp}\beta^\ell \neq \emptyset \\ \lambda_{\beta^k}(\hat{\beta}^\ell) \neq 0}} \text{supp}\hat{\beta}^k \Big), \tag{8}$$

where the coefficients $\lambda_{\beta^k}(\hat{\beta}^\ell)$ exist according to NNC. For non-zero coefficients $\lambda_{\hat{\beta}^k}(\hat{\beta}^\ell) = \lambda_{\beta^k}(\hat{\beta}^\ell) \neq 0$ it holds that the supports of $\hat{\beta}^k$ and $\hat{\beta}^\ell$ are nested, i.e., $\text{supp}\hat{\beta}^k \subseteq \text{supp}\hat{\beta}^\ell$. Therefore, the supports of the B-splines $\hat{\beta}^k$ in (8) are contained in the support of $\hat{\beta}^\ell$. Since also $\text{supp}\beta^\ell \subseteq \text{supp}\hat{\beta}^\ell$ we conclude that $\text{supp}\tilde{\beta}^\ell_{\mathcal{D}} \subseteq \text{supp}\hat{\beta}^\ell$. □

3. Assumptions and first results

Besides NNC, we impose two further assumptions in order to ensure good mathematical properties of the DPB-splines.

First, we introduce a condition that concerns the intersection of a patch B-spline with the constraining boundaries of lower levels. To be more precise, if a patch B-spline $\beta^n \in B^n$ does not vanish on a pair of constraining boundaries Γ^ℓ and Γ^k, where $\ell < n$ and $k < n$, then a non-empty intersection of the patch B-spline and the two constraining boundaries is assumed to exist, see also Fig. 7.

Assumption 2 (Intermediate Patch Condition – IPC)**.** *If* $\beta^n \in B^n$ *satisfies*

$$\text{supp}\beta^n \cap \Gamma^\ell \neq \emptyset,\ \ell < n \quad \textit{and} \quad \text{supp}\beta^n \cap \Gamma^k \neq \emptyset,\ k < n,$$

then

$$\text{supp}\beta^n \cap \Gamma^\ell \cap \Gamma^k \neq \emptyset.$$

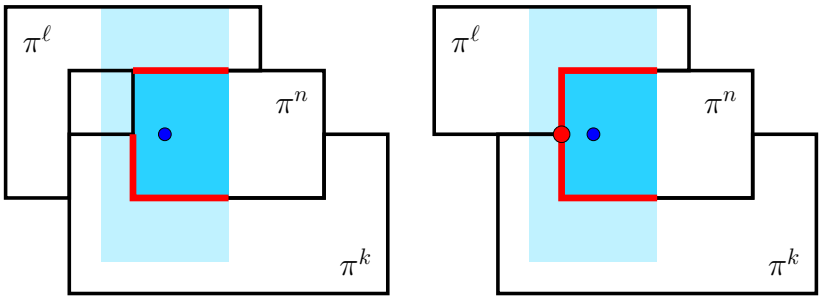

Figure 7: The intersection of a patch B-spline's support (dark blue) with Γ^ℓ and Γ^k is represented by the red line segments. The support of the associated extension $\hat{\beta}^n$ is also shown (light blue). IPC is violated in (a) and satisfied in (b).

The second assumption is needed to guarantee that the truncated basis functions are $C^{\mathbf{s}}$-smooth. We impose a condition on the intersection of a patch B-spline with a lower level constraining boundary, see Fig. 8.

Assumption 3 (Support Intersection Condition – SIC)**.** *The support of a patch B-spline* $\beta^n \in B^n$ *intersected with a constraining boundary* Γ^ℓ*,*

$$\text{supp}\beta^n \cap \Gamma^\ell,$$

where $\ell < n$*, is connected.*

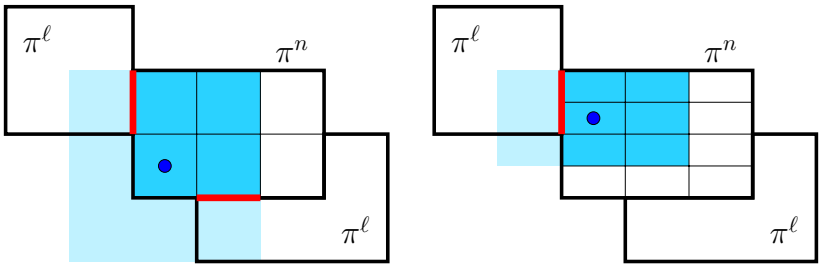

Figure 8: The intersection (red) of a patch B-spline's suppport (dark blue) with a constraining boundary Γ^ℓ, for $\ell < n$. SIC is violated in (a) and satisfied in (b).

In this and the following section, we assume that NNC, IPC and SIC are always satisfied. Eq. (3) implies that IPC and SIC are then also fulfilled for constraining boundaries $\Gamma^\ell_{\mathcal{D}}$ with respect to index sets $\mathcal{D}$, see (1). In the remainder of this section we discuss several technical results that can be derived from IPC and SIC. The four Lemmas build upon each other and allow us to analyze the smoothness of the PB-splines and the space that is spanned by them, see Fig. 9.

The first observation will help us to analyze the truncation defined in (6).

Lemma 2. *Two patch B-splines $\beta^k \in B^k$ and $\beta^\ell \in B^\ell$ with intersecting supports,*

$$\emptyset \neq \mathrm{supp}\beta^k \cap \mathrm{supp}\beta^\ell \subseteq \Gamma^\ell_{\mathcal{D}}, \text{ with } \ell < k \in \mathcal{D},$$

satisfy

$$\mathrm{supp}\beta^k \cap \Gamma^\ell_{\mathcal{D}} \subseteq \mathrm{supp}\beta^\ell \cap \Gamma^\ell_{\mathcal{D}}, \tag{9}$$

if $\lambda_{\beta^k}(\hat{\beta}^\ell) \neq 0$.

Proof. The existence of non-zero coefficients $\lambda_{\beta^k}(\hat{\beta}^\ell) \neq 0$ implies $\mathrm{supp}\beta^k \subseteq \mathrm{supp}\hat{\beta}^\ell$, hence

$$\mathrm{supp}\beta^k \cap \Gamma^\ell_{\mathcal{D}} \subseteq \mathrm{supp}\hat{\beta}^\ell \cap \Gamma^\ell_{\mathcal{D}}. \tag{10}$$

We distinguish between several cases: First, we assume that $\mathrm{supp}\hat{\beta}^\ell \cap \pi^\ell$ is connected. This leads immediately to (9) since $\beta^\ell = \hat{\beta}^\ell|_{\pi^\ell}$ and $\Gamma^\ell_{\mathcal{D}} \subseteq \pi^\ell$.

Second, we consider the case that $\mathrm{supp}\hat{\beta}^\ell \cap \pi^\ell$ possesses two connected components. Thus, besides β^ℓ, there exists another patch B-spline β'^ℓ such that $\mathrm{supp}\beta^\ell \cap \mathrm{supp}\beta'^\ell = \emptyset$ and

$$\mathrm{supp}\hat{\beta}^\ell \cap \pi^\ell = \mathrm{supp}\beta^\ell \cup \mathrm{supp}\beta'^\ell. \tag{11}$$

The intersection of $\mathrm{supp}\beta^k \cap \mathrm{supp}\beta^\ell$ belongs to the constraining boundary $\Gamma^\ell_{\mathcal{D}}$, thus

$$\emptyset \neq \mathrm{supp}\beta^k \cap \mathrm{supp}\beta^\ell = \mathrm{supp}\beta^k \cap \mathrm{supp}\beta^\ell \cap \Gamma^\ell_{\mathcal{D}}. \tag{12}$$

According to SIC and Eq. (3), $\mathrm{supp}\beta^k \cap \Gamma^\ell_{\mathcal{D}}$ is connected. Since the two parts $\mathrm{supp}\beta^\ell \cap \Gamma^\ell_{\mathcal{D}}$ and $\mathrm{supp}\beta'^\ell \cap \Gamma^\ell_{\mathcal{D}}$ of the constraining boundary are disjoint it follows that

$$\mathrm{supp}\beta^k \cap \mathrm{supp}\beta'^\ell \cap \Gamma^\ell_{\mathcal{D}} = \emptyset. \tag{13}$$

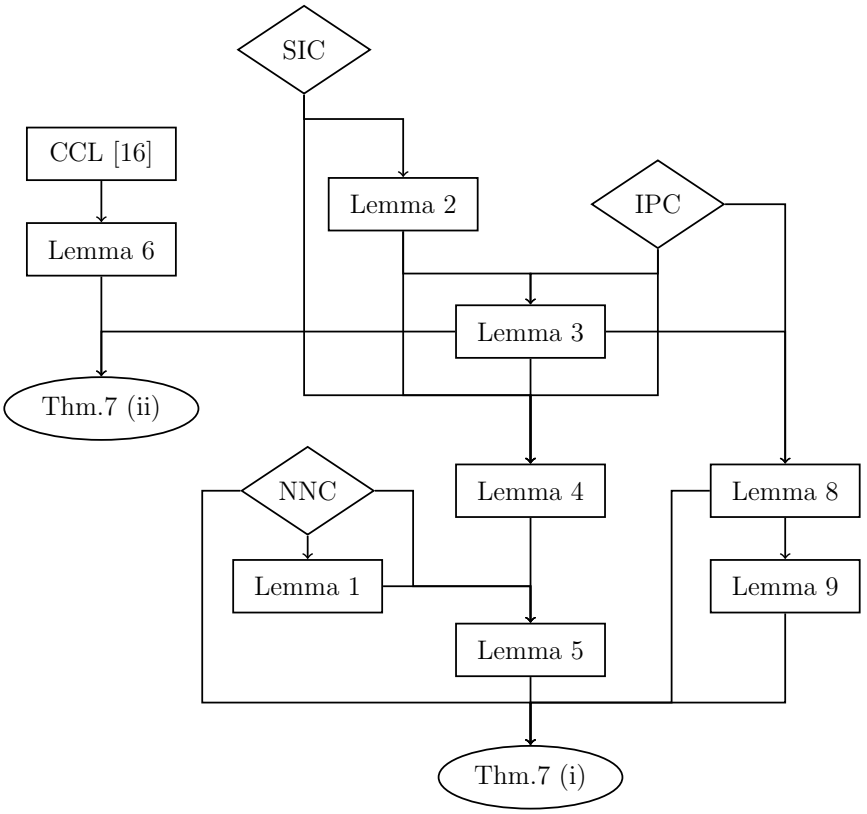

Figure 9: Diagram representing the connections between Assumptions (diamonds) , Lemmas (rectangles) and DPB-spline properties (ellipses).

We observe that (10) is equivalent to

$$(\text{supp}\beta^k \cap \Gamma_{\mathcal{D}}^{\ell}) \cap (\text{supp}\hat{\beta}^{\ell} \cap \Gamma_{\mathcal{D}}^{\ell}) = \text{supp}\beta^k \cap \Gamma_{\mathcal{D}}^{\ell}. \tag{14}$$

We use (11) $\Gamma_{\mathcal{D}}^{\ell} \subseteq \pi^{\ell}$ to rewrite the left-hand side of this equation as

$$\text{supp}\beta^k \cap \text{supp}\hat{\beta}^{\ell} \cap \Gamma_{\mathcal{D}}^{\ell} = \text{supp}\beta^k \cap (\text{supp}\beta^{\ell} \cup \text{supp}\beta'^{\ell}) \cap \Gamma_{\mathcal{D}}^{\ell}.$$

We simplify the result with the help of (12) and (13),

$$\text{supp}\beta^k \cap (\text{supp}\beta^{\ell} \cup \text{supp}\beta'^{\ell}) \cap \Gamma_{\mathcal{D}}^{\ell} = \text{supp}\beta^k \cap \text{supp}\beta^{\ell} \cap \Gamma_{\mathcal{D}}^{\ell}.$$

Therefore, (14) is equivalent to

$$(\text{supp}\beta^k \cap \Gamma_{\mathcal{D}}^{\ell}) \cap (\text{supp}\beta^{\ell} \cap \Gamma_{\mathcal{D}}^{\ell}) = \text{supp}\beta^k \cap \Gamma_{\mathcal{D}}^{\ell}.$$

This confirms that

$$\text{supp}\beta^k \cap \Gamma_{\mathcal{D}}^{\ell} \subseteq \text{supp}\beta^{\ell} \cap \Gamma_{\mathcal{D}}^{\ell}.$$

Finally we note that the proof in case two can be extended to more than two connected components. □

The next Lemma characterizes the intersection of a truncated patch B-spline $\tilde{\beta}^k_{\mathcal{D}}$, for $k \in \mathcal{D}$, with a lower level constraining boundary $\Gamma^\ell_{\mathcal{D}}$, see Fig. 10.

Lemma 3. *The truncated patch B-splines $\tilde{\beta}^k_{\mathcal{D}} \in T^k$ satisfy*

$$\mathrm{supp}\tilde{\beta}^k_{\mathcal{D}} \cap \Gamma^\ell_{\mathcal{D}} \neq \emptyset \;\Leftrightarrow \mathrm{supp}\beta^k \cap \Gamma^\ell_{\mathcal{D}} \neq \emptyset$$

if $k > \ell$ and $k \in \mathcal{D}$.

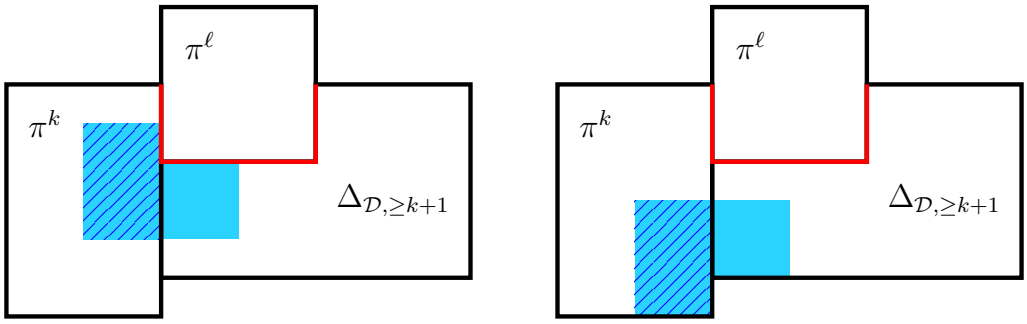

Figure 10: According to Lemma 3, the supports $\mathrm{supp}\beta^k$ (hatched blue) and $\mathrm{supp}\tilde{\beta}^k_{\mathcal{D}}$ (hatched blue and blue) either intersect both with $\Gamma^\ell_{\mathcal{D}}$ (red) or not, see (a) and (b), respectively.

Proof. According to the definition of the truncated functions, $\mathrm{supp}\beta^k \cap \Gamma^\ell_{\mathcal{D}} \neq \emptyset$ implies that $\mathrm{supp}\tilde{\beta}^k_{\mathcal{D}} \cap \Gamma^\ell_{\mathcal{D}} \neq \emptyset$. In order to prove the other implication, we assume that there exists a $\tilde{\beta}^k_{\mathcal{D}} \in T^k$ such that

$$\mathrm{supp}\tilde{\beta}^k_{\mathcal{D}} \cap \Gamma^\ell_{\mathcal{D}} \neq \emptyset, \quad \text{for } \ell < k,$$

but

$$\mathrm{supp}\beta^k \cap \Gamma^\ell_{\mathcal{D}} = \emptyset. \tag{15}$$

It follows that

$$\mathrm{supp}\tilde{\beta}^k_{\mathcal{D}} \cap (\Delta_{\mathcal{D},\geq k+1} \setminus \pi^k) \cap \Gamma^\ell_{\mathcal{D}} \neq \emptyset,$$

since $\tilde{\beta}^k_{\mathcal{D}}$ takes non-zero values only on the associated patch and on the subdomain $\Delta_{\mathcal{D},\geq k+1}$. Among all such functions we pick one where k is maximal. The representation

$$\tilde{\beta}^k_{\mathcal{D}} = \sum_{\substack{\tilde{\beta}^m_{\mathcal{D}} \in P^{k+1}_{\mathcal{D}} \\ \mathrm{supp}\beta^m \cap \mathrm{supp}\beta^k \neq \emptyset}} \lambda_{\beta^m}(\hat{\beta}^k)\, \tilde{\beta}^m_{\mathcal{D}} \quad \text{on } \Delta_{\mathcal{D},\geq k+1},$$

see (6), implies that there exists a function $\tilde{\beta}^m_{\mathcal{D}} \in P^{k+1}_{\mathcal{D}}$ with $\mathrm{supp}\beta^m \cap \mathrm{supp}\beta^k \neq \emptyset$ such that

$$\mathrm{supp}\tilde{\beta}^m_{\mathcal{D}} \cap \Gamma^\ell_{\mathcal{D}} \neq \emptyset.$$

It follows immediately that

$$\mathrm{supp}\beta^m \cap \Gamma^\ell_{\mathcal{D}} \neq \emptyset,$$

since k is the largest level with the property (15). Furthermore, $\text{supp}\beta^m \cap \text{supp}\beta^k \neq \emptyset$ implies that $\text{supp}\beta^m \cap \Gamma_{\mathcal{D}}^k \neq \emptyset$, and hence

$$\emptyset \neq \text{supp}\beta^m \cap \Gamma_{\mathcal{D}}^k \cap \Gamma_{\mathcal{D}}^\ell \subseteq \text{supp}\beta^k \cap \Gamma_{\mathcal{D}}^k \cap \Gamma_{\mathcal{D}}^\ell = \emptyset,$$

where the first equation holds according to IPC, the second statement follows from Lemma 2, and the last equality is obtained by (15). This is a contradiction. □

Lemma 3 enables us to reformulate the selection mechanism. More precisely, instead of considering the truncated patch B-spline $\tilde{\beta}_{\mathcal{D}}^k$ if suffices to analyze whether the associated patch B-spline β^k vanishes on the constraining boundary,

$$S_{\mathcal{D}}^{\ell+1} = \{\tilde{\beta}_{\mathcal{D}}^k \in P_{\mathcal{D}}^{\ell+1} \ : \ \beta^k = 0 \quad \text{on} \quad \Gamma_{\mathcal{D}}^\ell\}.$$

Next, we observe that the truncated patch B-splines $\tilde{\beta}_{\mathcal{D}}^k \in T^k$ inherit the support intersection property:

Lemma 4. *The intersections of the supports of truncated patch B-splines $\tilde{\beta}_{\mathcal{D}}^k \in T^k$ with constraining boundaries*

$$\text{supp}\tilde{\beta}_{\mathcal{D}}^k \cap \Gamma_{\mathcal{D}}^\ell \text{ where } \ell < k \tag{16}$$

are connected.

Proof. Assume there exists a truncated patch B-spline $\tilde{\beta}_{\mathcal{D}}^k$ whose support intersects the lower level constraining boundary $\Gamma_{\mathcal{D}}^\ell$ in more than one connected component. Among all those functions we choose one where $k \in \mathcal{D}$ is maximal. The intersection splits into two disjoint sets $\delta_1 \neq \emptyset$ and $\delta_2 \neq \emptyset$ with $\delta_1 \cap \delta_2 = \emptyset$ such that

$$\text{supp}\tilde{\beta}_{\mathcal{D}}^k \cap \Gamma_{\mathcal{D}}^\ell = \delta_1 \cup \delta_2. \tag{17}$$

SIC requires that $\text{supp}\beta^k \cap \Gamma_{\mathcal{D}}^\ell$ is connected. Since $\text{supp}\beta^k \subseteq \text{supp}\tilde{\beta}_{\mathcal{D}}^k$, this implies that $\text{supp}\beta^k \cap \Gamma_{\mathcal{D}}^\ell$ is a subset of one δ_i whereas its intersection with the other one is empty. Without loss of generality we assume

$$\text{supp}\beta^k \cap \Gamma_{\mathcal{D}}^\ell \subseteq \delta_1 \quad \text{and} \quad \text{supp}\beta^k \cap \delta_2 = \emptyset. \tag{18}$$

According to the latter observation, the truncated patch B-spline $\tilde{\beta}_{\mathcal{D}}^k$ intersects δ_2 in patches of levels higher than k, i.e.,

$$\text{supp}\tilde{\beta}_{\mathcal{D}}^k \cap (\Delta_{\mathcal{D},\geq k+1} \setminus \pi^k) \cap \delta_2 \neq \emptyset.$$

Due to the definition of the truncation (6), there exists a function $\tilde{\beta}_{\mathcal{D}}^m \in P_{\mathcal{D}}^{k+1}$ with $\text{supp}\beta^m \cap \text{supp}\beta^k \neq \emptyset$ that satisfies

$$\text{supp}\tilde{\beta}_{\mathcal{D}}^m \cap \delta_2 \neq \emptyset. \tag{19}$$

Moreover, we have

$$\text{supp}\tilde{\beta}_{\mathcal{D}}^m \cap \Gamma_{\mathcal{D}}^\ell \subseteq \text{supp}\tilde{\beta}_{\mathcal{D}}^k \cap \Gamma_{\mathcal{D}}^\ell = \delta_1 \cup \delta_2.$$

Recall that we assumed k to be maximal. Thus $\mathrm{supp}\tilde{\beta}^m_{\mathcal{D}} \cap \Gamma^\ell_{\mathcal{D}}$ is connected and we obtain

$$\mathrm{supp}\tilde{\beta}^m_{\mathcal{D}} \cap \delta_1 = \emptyset. \tag{20}$$

From $\mathrm{supp}\beta^m \cap \mathrm{supp}\beta^k \neq \emptyset$ it follows that $\mathrm{supp}\beta^m \cap \Gamma^k_{\mathcal{D}} \neq \emptyset$. Furthermore, (19) leads to

$$\emptyset \neq \mathrm{supp}\tilde{\beta}^m_{\mathcal{D}} \cap \delta_2 \subseteq \mathrm{supp}\tilde{\beta}^m_{\mathcal{D}} \cap \Gamma^\ell_{\mathcal{D}},$$

since (17) implies that $\delta_2 \subseteq \Gamma^\ell_{\mathcal{D}}$. According to Lemma 3 $\mathrm{supp}\tilde{\beta}^m_{\mathcal{D}} \cap \Gamma^\ell_{\mathcal{D}} \neq \emptyset$ is equivalent to $\mathrm{supp}\beta^m \cap \Gamma^\ell_{\mathcal{D}} \neq \emptyset$. Applying IPC leads to

$$\mathrm{supp}\beta^m \cap \Gamma^k_{\mathcal{D}} \cap \Gamma^\ell_{\mathcal{D}} \neq \emptyset.$$

Furthermore, Lemma 2 states that $\mathrm{supp}\beta^m \cap \Gamma^k_{\mathcal{D}} \subseteq \mathrm{supp}\beta^k \cap \Gamma^k_{\mathcal{D}}$. Combining these observations with simple subset relations and (18) results in the following equations,

$$\emptyset \neq \mathrm{supp}\beta^m \cap \Gamma^k_{\mathcal{D}} \cap \Gamma^\ell_{\mathcal{D}} \subseteq \mathrm{supp}\beta^k \cap \Gamma^k_{\mathcal{D}} \cap \Gamma^\ell_{\mathcal{D}} \subseteq \mathrm{supp}\beta^k \cap \Gamma^\ell_{\mathcal{D}} \subseteq \delta_1.$$

However, this implies that

$$\emptyset \neq \mathrm{supp}\beta^m \cap \delta_1 \subseteq \mathrm{supp}\tilde{\beta}^m_{\mathcal{D}} \cap \delta_1,$$

which contradicts, (20), and thereby concluding the proof. □

Finally we present an extension of Lemma 2.

Lemma 5. *The supports of truncated patch B-splines $\tilde{\beta}^k_{\mathcal{D}} \in P^{\ell+1}_{\mathcal{D}}$ and patch B-splines $\beta^\ell \in B^\ell$ of lower level $\ell < k$ satisfy*

$$\mathrm{supp}\tilde{\beta}^k_{\mathcal{D}} \cap \Gamma^\ell_{\mathcal{D}} \subseteq \mathrm{supp}\beta^\ell \cap \Gamma^\ell_{\mathcal{D}},$$

if $\mathrm{supp}\beta^k \cap \mathrm{supp}\beta^\ell \neq \emptyset$ *and* $\lambda_{\beta^k}(\hat{\beta}^\ell) \neq 0$.

Proof. The proof works similar to the proof of Lemma 2. We do not provide all details but show how to adapt it to the current situation.

Recall that $\lambda_{\beta^k}(\hat{\beta}^\ell) \neq 0$ implies $\mathrm{supp}\hat{\beta}^k \subseteq \mathrm{supp}\hat{\beta}^\ell$. From Lemma 1 it follows that $\mathrm{supp}\tilde{\beta}^k_{\mathcal{D}} \subseteq \mathrm{supp}\hat{\beta}^\ell$ and thus,

$$\mathrm{supp}\tilde{\beta}^k_{\mathcal{D}} \cap \Gamma^\ell_{\mathcal{D}} \subseteq \mathrm{supp}\hat{\beta}^\ell \cap \Gamma^\ell_{\mathcal{D}}.$$

As in Lemma 2, the proof follows immediately for the case that $\mathrm{supp}\hat{\beta}^\ell \cap \pi^\ell$ possesses one connected component. For the other case we note that

$$\emptyset \neq \mathrm{supp}\beta^k \cap \mathrm{supp}\beta^\ell \cap \Gamma^\ell_{\mathcal{D}} \subseteq \mathrm{supp}\tilde{\beta}^k_{\mathcal{D}} \cap \mathrm{supp}\beta^\ell \cap \Gamma^\ell_{\mathcal{D}},$$

according to the assumption that $\mathrm{supp}\beta^k \cap \mathrm{supp}\beta^\ell \neq \emptyset$. Using Lemma 4 allows us to proceed as in the proof of Lemma 2 using $\tilde{\beta}^k_{\mathcal{D}}$ instead of β^k. □

4. Space characterization

Before investigating the mathematical properties of the DPB-splines we introduce the notion of *homogenous boundary conditions*.

A $C^{\mathbf{s}}$–smooth function f satisfies homogeneous boundary conditions in a point $\mathbf{x}$ if the values of the function and of all its partial derivatives up to order $s_k = p_k - 1$ in all variables separately[3] are equal to zero,

$$\vartheta f(\mathbf{x}) = 0,$$

with

$$[\vartheta f(\mathbf{x})]_{\mathbf{i}} = \partial_{\mathbf{i}} f(\mathbf{x}), \quad \mathbf{i} = (i_1, \ldots, i_d), \quad i_k \leq p_k - 1.$$

and partial derivative operators

$$(\partial_{\mathbf{i}} f)(\mathbf{x}) = \frac{\partial^{i_1}}{\partial x_1^{i_1}} \cdots \frac{\partial^{i_d}}{\partial x_d^{i_d}} f(x_1, \ldots, x_d).$$

The knot hyperplanes of the space $\mathbb{V}^\ell$ divide the patch π^ℓ into cells $z \in Z^\ell$, where Z^ℓ denotes the set of all cells of level ℓ. Therefore, the boundary of a patch π^ℓ naturally splits into facets ξ of different dimensions. E.g., the facets can be edges or vertices of cells of level ℓ for dimension $d = 2$, see also the Appendix of [40].

Lemma 6. *If a function $f \in \mathbb{V}^\ell$ satisfies homogeneous boundary conditions on a boundary facet ξ of π^ℓ, then $\lambda_{\beta^\ell}(f) = 0$ if $\xi \subseteq \mathrm{supp}\beta^\ell$.*

Proof. We note that for a cell $z \in Z^\ell$ and every $\beta^\ell \in B^\ell$ that does not vanish on that cell, i.e., $z \subseteq \mathrm{supp}\beta^\ell$, it holds that

$$0 \neq \beta^\ell|_z = \hat{\beta}^\ell|_z,$$

according to (4). Suitably adapting the proof of Lemma 2 in [40], which is based on the Contact Characterization Lemma (CCL) in [16], confirms this fact. □

The following theorem shows that the DPB-splines form a basis and characterizes the space that is spanned by them.

Theorem 7. *We consider DPB-splines $P_{\mathcal{D}}$ on any subdomain $\Delta_{\mathcal{D}} \subseteq \Omega$.*

(i) The functions $\tilde{\beta}^\ell_{\mathcal{D}} \in P_{\mathcal{D}}$ possess continuous values and partial derivatives up to order $p - 1$ in each variable separately.

(ii) The DPB-splines form a basis of the patchwork spline space $\mathbb{P}_{\mathcal{D}}$.

(iii) The DPB-splines satisfy the coefficient preservation property, i.e., for any function $f \in \mathbb{P}_{\mathcal{D}}$ it holds that

$$f = \sum_{\tilde{\beta}^k_{\mathcal{D}} \in P_{\mathcal{D}}} \lambda_{\beta^k}(f)\, \tilde{\beta}^k_{\mathcal{D}}, \quad \text{on } \Delta_{\mathcal{D}}. \tag{21}$$

[3]For instance, $f = f_x = f_y = f_{xx} = f_{xy} = f_{yy} = f_{xxy} = f_{xyy} = f_{xxyy} = 0$ for $\mathbf{x} = (x, y)$ and $\mathbf{s} = (2, 2)$.

(iv) The DPB-spline functions are non-negative and form a partition of unity.

Proof. We prove the above statements for all subdomains $\Delta_{\mathcal{D}} \subseteq \Delta_{\geq \ell}$, i.e., $\mathcal{D} \subseteq \{\ell, \dots, N\}$, by induction over ℓ, proceeding from the maximum level N down to 1.

For $\ell = N$ we note that $\Delta_{\geq N} = \pi^N$. Therefore, a subdomain of $\Delta_{\geq N}$ is either the empty set (trivial case) or $\mathcal{D} = \{N\}$. Then $P_{\mathcal{D}} = T^N_{\mathcal{D}}$ consists of functions

$$\tilde{\beta}^N_{\mathcal{D}} = \begin{cases} \beta^N & \text{on } \pi^N \\ 0 & \text{elsewhere} \end{cases}.$$

Therefore, we can conclude that (i)-(iv) are satisfied for any subdomain $\Delta_{\mathcal{D}} \subseteq \Delta_{\geq N}$.

Now we assume that (i)-(iv) are satisfied for any subdomain $\Delta_{\mathcal{D}} \subseteq \Delta_{\geq \ell+1}$. We show that the properties extend to any subdomain $\Delta_{\mathcal{D}} \subseteq \Delta_{\geq \ell}$. We consider only the case where $\ell \in \mathcal{D}$, hence $\mathcal{D} \subseteq \{\ell, \dots, N\}$. Otherwise, the result follows immediately from the induction hypothesis.

(i) We have that

$$P_{\mathcal{D}} = P^1_{\mathcal{D}} = P^\ell_{\mathcal{D}} = T^\ell_{\mathcal{D}} \cup S^{\ell+1}_{\mathcal{D}}.$$

For functions in $S^{\ell+1}_{\mathcal{D}}$ the smoothness on $\Delta_{\mathcal{D}} = \Delta_{\mathcal{D},\geq \ell}$ follows from the induction hypothesis combined with the fact that the functions are zero on π^ℓ and satisfy homogeneous boundary conditions on $\Gamma^\ell_{\mathcal{D}}$ according to the selection mechanism. Next we consider a function $\tilde{\beta}^\ell_{\mathcal{D}} \in T^\ell_{\mathcal{D}}$. We note that $\tilde{\beta}^\ell_{\mathcal{D}}$ obviously possesses the required smoothness on π^ℓ and also on $\Delta_{\mathcal{D},\geq \ell+1} \setminus \pi^\ell$ (considered separately). Indeed, its restriction to the latter domain is a linear combination of functions in $P^{\ell+1}_{\mathcal{D}}$, which satisfy the smoothness conditions according to the induction hypothesis.

Now it remains to be shown that $\tilde{\beta}^\ell_{\mathcal{D}}$ possesses the required order of smoothness on the constraining boundary $\Gamma^\ell_{\mathcal{D}}$. According to NNC it holds that $\hat{\beta}^\ell \in \mathbb{P}_{\mathcal{N}^\ell_{\mathcal{D}}}$. From the induction hypothesis (ii) it follows that there exists a representation,

$$\hat{\beta}^\ell = \sum_{\tilde{\beta}^k_{\mathcal{N}^\ell_{\mathcal{D}}} \in P_{\mathcal{N}^\ell_{\mathcal{D}}}} \lambda_{\beta^k}(\hat{\beta}^\ell) \tilde{\beta}^k_{\mathcal{N}^\ell_{\mathcal{D}}} \quad \text{on } \Delta_{\mathcal{N}^\ell_{\mathcal{D}}}.$$

We use it to define the auxiliary function

$$\hat{\beta}^\ell_{\mathcal{N}^\ell_{\mathcal{D}}} = \sum_{\substack{\tilde{\beta}^k_{\mathcal{N}^\ell_{\mathcal{D}}} \in P_{\mathcal{N}^\ell_{\mathcal{D}}} \\ \text{supp}\beta^k \cap \text{supp}\beta^\ell \neq \emptyset}} \lambda_{\beta^k}(\hat{\beta}^\ell) \tilde{\beta}^k_{\mathcal{N}^\ell_{\mathcal{D}}}, \tag{22}$$

by considering only functions near the boundary to $\text{supp}\beta^\ell$ and observe that

$$\vartheta \hat{\beta}^\ell_{\mathcal{N}^\ell_{\mathcal{D}}} = \vartheta \hat{\beta}^\ell = \vartheta \beta^\ell \quad \text{on } \Gamma^\ell_{\mathcal{D}} \cap \text{supp}\beta^\ell.$$

Furthermore, it holds that

$$\vartheta \hat{\beta}^\ell_{\mathcal{N}^\ell_{\mathcal{D}}} = \vartheta \beta^\ell = 0 \quad \text{on } \Gamma^\ell_{\mathcal{D}} \setminus \text{supp}\beta^\ell,$$

since $\mathrm{supp}\tilde{\beta}^k_{\mathcal{N}^\ell_\mathcal{D}} \cap \Gamma^\ell_{\mathcal{N}^\ell_\mathcal{D}} \subseteq \mathrm{supp}\beta^\ell \cap \Gamma^\ell_{\mathcal{N}^\ell_\mathcal{D}}$ according to Lemma 5 and $\Gamma^\ell_{\mathcal{N}^\ell_\mathcal{D}} = \Gamma^\ell_\mathcal{D}$. Therefore, we obtain that $\vartheta\hat{\beta}^\ell_{\mathcal{N}^\ell_\mathcal{D}} = \vartheta\beta^\ell$ on $\Gamma^\ell_\mathcal{D}$.

Now we show that the auxiliary function shares values and derivatives with the truncated function along the constraining boundary, $\vartheta\hat{\beta}^\ell_{\mathcal{N}^\ell_\mathcal{D}} = \vartheta\tilde{\beta}^\ell_\mathcal{D}$ on $\Gamma^\ell_\mathcal{D}$. More precisely, we prove that

$$\vartheta\Big(\sum_{\substack{\tilde{\beta}^k_{\mathcal{N}^\ell_\mathcal{D}} \in P_{\mathcal{N}^\ell_\mathcal{D}} \\ \mathrm{supp}\beta^k \cap \mathrm{supp}\beta^\ell \neq \emptyset}} \lambda_{\beta^k}(\hat{\beta}^\ell)\tilde{\beta}^k_{\mathcal{N}^\ell_\mathcal{D}}\Big) = \vartheta\Big(\sum_{\substack{\tilde{\beta}^k_\mathcal{D} \in P^{\ell+1}_\mathcal{D} \\ \mathrm{supp}\beta^k \cap \mathrm{supp}\beta^\ell \neq \emptyset}} \lambda_{\beta^k}(\hat{\beta}^\ell)\tilde{\beta}^k_\mathcal{D}\Big), \quad \text{on } \Gamma^\ell_\mathcal{D}. \tag{23}$$

We note that

$$\mathrm{supp}\beta^k \cap \mathrm{supp}\beta^\ell \neq \emptyset \;\Rightarrow\; \beta^k|_{\Gamma^\ell_\mathcal{D}} \neq 0, \quad \text{if } k > \ell.$$

The proof of (23) is based on two technical Lemmas. The first one states that the selection mechanism always selectes the same functions for $\mathcal{D}$ and $\mathcal{N}^\ell_\mathcal{D}$.

Lemma 8. *For all $\beta^k \in B^k$ with $\beta^k \neq 0$ on $\Gamma^\ell_\mathcal{D}$ it holds that*

$$\tilde{\beta}^k_{\mathcal{N}^\ell_\mathcal{D}} \in P^m_{\mathcal{N}^\ell_\mathcal{D}} \Leftrightarrow \tilde{\beta}^k_\mathcal{D} \in P^m_\mathcal{D}, \tag{24}$$

if $k \geq m > \ell$.

Proof. On the one hand, we consider a function $\tilde{\beta}^k_\mathcal{D} \in P^m_\mathcal{D}$ with $\mathrm{supp}\beta^k \cap \Gamma^\ell_\mathcal{D} \neq \emptyset$. Hence, $k \in \mathcal{N}^\ell_\mathcal{D}$. We note that

$$P^m_\mathcal{D} = \bigcup_{k\in\mathcal{D}, k\geq m} \{\tilde{\beta}^k_\mathcal{D} \in T^k_\mathcal{D} \;:\; \mathrm{supp}\beta^k \cap \Gamma^r_\mathcal{D} = \emptyset, \quad \text{for all } r \in \mathcal{D},\ m \leq r < k\} \tag{25}$$

and

$$P^m_{\mathcal{N}^\ell_\mathcal{D}} = \bigcup_{k\in\mathcal{N}^\ell_\mathcal{D}, k\geq m} \{\tilde{\beta}^k_{\mathcal{N}^\ell_\mathcal{D}} \in T^k_{\mathcal{N}^\ell_\mathcal{D}} \;:\; \mathrm{supp}\beta^k \cap \Gamma^r_{\mathcal{N}^\ell_\mathcal{D}} = \emptyset, \quad \text{for all } r \in \mathcal{N}^\ell_\mathcal{D},\ m \leq r < k\},$$

according to the selection mechanism and Lemma 3. Since $\Gamma^r_{\mathcal{N}^\ell_\mathcal{D}} \subseteq \Gamma^r_\mathcal{D}$ for $r \in \mathcal{N}^\ell_\mathcal{D}$, the first condition $\mathrm{supp}\beta^k \cap \Gamma^r_\mathcal{D} = \emptyset$ implies $\mathrm{supp}\beta^k \cap \Gamma^r_{\mathcal{N}^\ell_\mathcal{D}} = \emptyset$ if $m \leq r < k$. Therefore, we conclude that $\tilde{\beta}^k_{\mathcal{N}^\ell_\mathcal{D}} \in P^m_{\mathcal{N}^\ell_\mathcal{D}}$.

On the other hand, assume there exists a function $\tilde{\beta}^k_{\mathcal{N}^\ell_\mathcal{D}} \in P^m_{\mathcal{N}^\ell_\mathcal{D}}$ with $\tilde{\beta}^k_\mathcal{D} \notin P^m_\mathcal{D}$ and $\beta^k \neq 0$ on $\Gamma^\ell_\mathcal{D}$. We invoke the characterization (25) to conclude that there exists a level $r \in \mathcal{D} \setminus \mathcal{N}^\ell_\mathcal{D}$ and $m \leq r < k$ such that $\mathrm{supp}\beta^k \cap \Gamma^r_\mathcal{D} \neq \emptyset$. The considered function satisfies $\mathrm{supp}\beta^k \cap \Gamma^\ell_\mathcal{D} \neq \emptyset$ and hence it follows that $\mathrm{supp}\beta^k \cap \Gamma^\ell_\mathcal{D} \cap \Gamma^r_\mathcal{D} \neq \emptyset$ by IPC. However, since π^r is not a neighbor of π^ℓ it holds that $\Gamma^r_\mathcal{D} \cap \Gamma^\ell_\mathcal{D} \subseteq \pi^r \cap \pi^\ell = \emptyset$ which implies that $\mathrm{supp}\beta^k \cap \Gamma^\ell_\mathcal{D} \cap \Gamma^r_\mathcal{D} = \emptyset$. This is a contradiction. □ Lem.8

The second lemma confirms that the functions considered in the previous lemma possess the same values and derivatives along the constraining boundary.

Lemma 9. *For all functions in* (24) *with* $\tilde{\beta}^k_{\mathcal{D}} \in P^m_{\mathcal{D}}$ *it holds that*

$$\vartheta\tilde{\beta}^k_{\mathcal{D}} = \vartheta\tilde{\beta}^k_{\mathcal{N}^\ell_{\mathcal{D}}} \quad \text{on } \Gamma^\ell_{\mathcal{D}} \cap \Delta_{\mathcal{D},\geq m}, \tag{26}$$

if $k \geq m > \ell$.

Proof. We use induction over the level m from n down to $\ell+1$ with $n = \max\{k \in \mathcal{N}^\ell_{\mathcal{D}}\}$. It suffices to consider these functions since levels higher than n are not active on $\Gamma^\ell_{\mathcal{D}}$.

For level n it holds that

$$\tilde{\beta}^n_{\mathcal{D}} = \beta^n = \tilde{\beta}^n_{\mathcal{N}^\ell_{\mathcal{D}}}, \quad \text{on } \pi^n,$$

for all $\tilde{\beta}^n_{\mathcal{D}} \in P^n_{\mathcal{D}}$. Thus, $\vartheta\tilde{\beta}^n_{\mathcal{D}} = \vartheta\tilde{\beta}^n_{\mathcal{N}^\ell_{\mathcal{D}}}$ on $\Gamma^\ell_{\mathcal{D}} \cap \Delta_{\mathcal{D},\geq n}$. In order to complete the proof by induction, we assume that (26) is satisfied for $m+1$ and show that this extends to m.

First, we consider functions $\tilde{\beta}^k_{\mathcal{D}} \in P^m_{\mathcal{D}}$ with $k > m$. The induction hypothesis implies that

$$\vartheta\tilde{\beta}^k_{\mathcal{D}} = \vartheta\tilde{\beta}^k_{\mathcal{N}^\ell_{\mathcal{D}}}, \quad \text{on } \Gamma^\ell_{\mathcal{D}} \cap \Delta_{\mathcal{D},\geq m+1}.$$

Furthermore, the selection ensures that these functions vanish on π^m, hence

$$\vartheta\tilde{\beta}^k_{\mathcal{D}} = \vartheta\tilde{\beta}^k_{\mathcal{N}^\ell_{\mathcal{D}}} = 0, \quad \text{on } \Gamma^\ell_{\mathcal{D}} \cap \pi^m.$$

The equality on $\Gamma^\ell_{\mathcal{D}} \cap \Delta_{\mathcal{D},\geq m}$ now follows from

$$\Gamma^\ell_{\mathcal{D}} \cap \Delta_{\mathcal{D},\geq m} = (\Gamma^\ell_{\mathcal{D}} \cap \pi^m) \cup (\Gamma^\ell_{\mathcal{D}} \cap \Delta_{\mathcal{D},\geq m+1}). \tag{27}$$

Second, we consider the remaining functions $\tilde{\beta}^m_{\mathcal{D}} \in T^m_{\mathcal{D}}$. Obviously, it holds that

$$\vartheta\tilde{\beta}^m_{\mathcal{D}} = \vartheta\tilde{\beta}^m_{\mathcal{N}^\ell_{\mathcal{D}}} = \vartheta\beta^m, \quad \text{on } \Gamma^\ell_{\mathcal{D}} \cap \pi^m.$$

Furthermore,

$$\tilde{\beta}^m_{\mathcal{D}} = \sum_{\substack{\tilde{\beta}^r_{\mathcal{D}} \in P^{m+1}_{\mathcal{D}} \\ \operatorname{supp}\beta^r \cap \operatorname{supp}\beta^m \neq \emptyset}} \lambda_{\beta^r}(\hat{\beta}^m)\tilde{\beta}^r_{\mathcal{D}} \quad \text{on } \Delta_{\mathcal{D},\geq m+1}.$$

The previous lemma (see (24)) and the induction hypothesis imply

$$\vartheta\Big(\sum_{\substack{\tilde{\beta}^r_{\mathcal{D}} \in P^{m+1}_{\mathcal{D}} \\ \operatorname{supp}\beta^r \cap \operatorname{supp}\beta^m \neq \emptyset}} \lambda_{\beta^r}(\hat{\beta}^m)\tilde{\beta}^r_{\mathcal{D}}\Big) = \vartheta\Big(\sum_{\substack{\tilde{\beta}^r_{\mathcal{N}^\ell_{\mathcal{D}}} \in P^{m+1}_{\mathcal{N}^\ell_{\mathcal{D}}} \\ \operatorname{supp}\beta^r \cap \operatorname{supp}\beta^m \neq \emptyset}} \lambda_{\beta^r}(\hat{\beta}^m)\tilde{\beta}^r_{\mathcal{N}^\ell_{\mathcal{D}}}\Big) = \vartheta\tilde{\beta}^m_{\mathcal{N}^\ell_{\mathcal{D}}} \quad \text{on } \Gamma^\ell_{\mathcal{D}} \cap \Delta_{\mathcal{D},\geq m+1}.$$

Invoking the decomposition (27) confirms that (26) is satisfied for all $\tilde{\beta}^m_{\mathcal{D}} \in T^m_{\mathcal{D}}$. $\square_{\text{Lem.9}}$

Now we are able to prove the original statement (23). Applying both Lemmas with $m = \ell+1$ confirms that $\vartheta\hat{\beta}^\ell_{\mathcal{N}^\ell_{\mathcal{D}}} = \vartheta\beta^\ell = \vartheta\tilde{\beta}^\ell_{\mathcal{D}}$ on $\Gamma^\ell_{\mathcal{D}} = \Gamma^\ell_{\mathcal{D}} \cap \Delta_{\mathcal{D},\geq\ell}$ since $P_{\mathcal{N}^\ell_{\mathcal{D}}} = P^1_{\mathcal{N}^\ell_{\mathcal{D}}} = P^{\ell+1}_{\mathcal{N}^\ell_{\mathcal{D}}}$. Hence, we conclude that the functions $\tilde{\beta}^\ell_{\mathcal{D}} \in T^\ell_{\mathcal{D}}$ possess the required order of smoothness on $\Delta_{\mathcal{D},\geq\ell}$.

(ii) We consider a function $f \in \mathbb{P}_{\mathcal{D}}$. Its restriction to π^ℓ has a representation

$$f = \sum_{\beta^\ell \in B^\ell} \lambda_{\beta^\ell}(f)\, \beta^\ell = \sum_{\beta^\ell \in B^\ell} \lambda_{\beta^\ell}(f)\, \tilde{\beta}^\ell_{\mathcal{D}} \quad \text{on } \pi^\ell, \tag{28}$$

since $\beta^\ell = \tilde{\beta}^\ell_{\mathcal{D}}$ on π^ℓ. We now define

$$\tilde{f} = f - \sum_{\beta^\ell \in B^\ell} \lambda_{\beta^\ell}(f)\, \tilde{\beta}^\ell_{\mathcal{D}} \quad \text{on } \Delta_{\mathcal{D}}. \tag{29}$$

Clearly, $\tilde{f}$ is equal to zero on π^ℓ and satisfies homogeneous boundary conditions on $\Gamma^\ell_{\mathcal{D}}$. We observe that $\tilde{f} \in \mathbb{P}^{\ell+1}_{\mathcal{D}}$. Indeed, the definition of the patchwork spline space $\mathbb{P}_{\mathcal{D}}$ gives $f \in \mathbb{P}^{\ell+1}_{\mathcal{D}}$, and the functions $\tilde{\beta}^\ell_{\mathcal{D}} \in T^\ell_{\mathcal{D}}$ are linear combinations of functions in $\mathbb{P}^{\ell+1}_{\mathcal{D}}$. According to the induction hypothesis there exists a representation

$$\tilde{f} = \sum_{\tilde{\beta}^k_{\mathcal{D}} \in P^{\ell+1}_{\mathcal{D}}} \lambda_{\beta^k}(\tilde{f})\, \tilde{\beta}^k_{\mathcal{D}} \quad \text{on } \Delta_{\mathcal{D},\geq \ell+1}. \tag{30}$$

We consider a function $\tilde{\beta}^k_{\mathcal{D}} \in P^{\ell+1}_{\mathcal{D}} \setminus S^{\ell+1}_{\mathcal{D}}$ in the above sum. The definition of $S^{\ell+1}_{\mathcal{D}}$ and Lemma 3 imply that

$$\mathrm{supp}\beta^k \cap \Gamma^\ell_{\mathcal{D}} \neq \emptyset.$$

There exists a facet ξ of $\pi^k \cap \pi^\ell \subseteq \Gamma^\ell_{\mathcal{D}}$ with $\xi \subseteq \mathrm{supp}\beta^k$ where $\tilde{f}$ satisfies the homogeneous boundary conditions. Therefore, we can apply Lemma 6 and obtain that $\lambda_{\beta^k}(\tilde{f}) = 0$.

Consequently, only functions in $S^{\ell+1}_{\mathcal{D}}$ contribute to the representation in (30) and thus, we can extend this representation to $\Delta_{\mathcal{D}}$,

$$\tilde{f} = \sum_{\tilde{\beta}^k_{\mathcal{D}} \in S^{\ell+1}_{\mathcal{D}}} \lambda_{\beta^k}(\tilde{f})\, \tilde{\beta}^k_{\mathcal{D}} \quad \text{on } \Delta_{\mathcal{D}}. \tag{31}$$

Therefore, we can combine equations (29) and (31) to represent f with respect to $P_{\mathcal{D}}$ on $\Delta_{\mathcal{D}}$,

$$f = \sum_{\tilde{\beta}^k \in P_{\mathcal{D}}} \mu_{\tilde{\beta}^k_{\mathcal{D}}}(f)\, \tilde{\beta}^k_{\mathcal{D}} \quad \text{on } \Delta_{\mathcal{D}}, \tag{32}$$

with coefficients

$$\mu_{\tilde{\beta}^k_{\mathcal{D}}}(f) = \begin{cases} \lambda_{\beta^\ell}(f) & \text{if } k = \ell \\ \lambda_{\beta^k}(\tilde{f}) & \text{otherwise.} \end{cases}$$

Finally, we note that the functions in $P_{\mathcal{D}}$ are linearly independent. Indeed, $T^\ell_{\mathcal{D}}$ is linearly independent on π^ℓ, since $\tilde{\beta}^\ell_{\mathcal{D}} = \beta^\ell$ on π^ℓ and the functions β^ℓ are linearly independent on π^ℓ. Moreover, the remaining functions in $S^{\ell+1}_{\mathcal{D}} \subseteq P^{\ell+1}_{\mathcal{D}}$ vanish on π^ℓ while being linearly independent on $\Delta_{\mathcal{D},\geq \ell+1}$ according to the induction hypothesis.

(iii) We rewrite Equation (32) by using the definition of the DPB-splines $P_{\mathcal{D}}$ and obtain

$$f = \sum_{\tilde{\beta}^\ell_{\mathcal{D}} \in T^\ell_{\mathcal{D}}} \mu_{\tilde{\beta}^\ell_{\mathcal{D}}}(f)\, \tilde{\beta}^\ell_{\mathcal{D}} + \sum_{\tilde{\beta}^k_{\mathcal{D}} \in S^{\ell+1}_{\mathcal{D}}} \mu_{\tilde{\beta}^k_{\mathcal{D}}}(f)\, \tilde{\beta}^k_{\mathcal{D}} \quad \text{on } \Delta_{\mathcal{D}}. \tag{33}$$

This confirms (21) with respect to the patch B-splines on π^ℓ since $\mu_{\tilde{\beta}^\ell_\mathcal{D}}(f) = \lambda_{\beta^\ell}(f)$.

Next we consider the restriction of f to $\Delta_{\mathcal{D},\geq\ell+1}$. On the one hand, it satisfies

$$f = \sum_{\tilde{\beta}^k_\mathcal{D} \in P^{\ell+1}_\mathcal{D}} \lambda_{\beta^k}(f)\, \tilde{\beta}^k_\mathcal{D} \quad \text{on } \Delta_{\mathcal{D},\geq\ell+1}, \tag{34}$$

according to the induction hypothesis (ii). On the other hand, we may rewrite (33) as

$$f = \underbrace{\sum_{\tilde{\beta}^\ell_\mathcal{D} \in T^\ell_\mathcal{D}} \lambda_{\beta^\ell}(f) \sum_{\substack{\tilde{\beta}^k_\mathcal{D} \in P^{\ell+1}_\mathcal{D} \\ \mathrm{supp}\beta^\ell \cap \mathrm{supp}\beta^k \neq \emptyset}} \lambda_{\beta^k}(\hat{\beta}^\ell)\, \tilde{\beta}^k_\mathcal{D}}_{(\star)} + \sum_{\tilde{\beta}^k_\mathcal{D} \in S^{\ell+1}_\mathcal{D}} \mu_{\tilde{\beta}^k_\mathcal{D}}(f)\, \tilde{\beta}^k_\mathcal{D} \quad \text{on } \Delta_{\mathcal{D},\geq\ell+1},$$

according to the definition of the truncation operator. Note that none of the functions $\tilde{\beta}^k_\mathcal{D}$ that appear in the double sum $(\star)$ belong to the set $S^{\ell+1}_\mathcal{D}$ of selected functions, since $\mathrm{supp}\beta^\ell \cap \mathrm{supp}\beta^k \neq \emptyset$ implies that $\beta^k \neq 0$ on $\Gamma^\ell_\mathcal{D}$. Therefore, comparing the coefficients with (34) confirms that $\mu_{\tilde{\beta}^k_\mathcal{D}}(f) = \lambda_{\beta^k}(f)$ for $\tilde{\beta}^k_\mathcal{D} \in S^{\ell+1}_\mathcal{D}$.

(iv) First, we show that the basis functions in $P^\ell_\mathcal{D} = T^\ell_\mathcal{D} \cup S^{\ell+1}_\mathcal{D}$ are non-negative on $\Delta_\mathcal{D}$. Since $S^{\ell+1}_\mathcal{D} \subseteq P^{\ell+1}_\mathcal{D}$ the induction hypothesis implies that functions in $S^{\ell+1}_\mathcal{D}$ are non-negative on $\Delta_{\mathcal{D},\geq\ell+1}$. This extends to $\Delta_\mathcal{D}$ as these functions vanish on π^ℓ according to the selection mechanism. The functions in $T^\ell_\mathcal{D}$ are non-negative on π^ℓ since there $\tilde{\beta}^\ell_\mathcal{D} = \beta^\ell$ and the functions β^ℓ are non-negative. Moreover, their representation with respect to $P^{\ell+1}_\mathcal{D} \setminus S^{\ell+1}_\mathcal{D}$ on $\Delta_{\mathcal{D},\geq\ell+1}$ is a linear combination of non-negative functions with non-negative coefficients.

Second, we note that the partition of unity is obtained by applying (21) to the function $f = 1$. $\square_{\text{Thm.7}}$

In addition to the patchwork spline space $\mathbb{P}_\mathcal{D}$ we consider the full spline space

$$\mathbb{F}_\mathcal{D} = \{f \in C^{\mathbf{s}}(\Delta_\mathcal{D}) \ : \ f|_z \in \Pi^{\mathbf{p}} \quad \forall z \in Z^\ell,\ \ell \in \mathcal{D}\},$$

where $\Pi^{\mathbf{p}}$ is the space of tensor-product polynomials of degree $\mathbf{p}$. We obtain the following result:

Corollary 10. *The DPB-splines $P_\mathcal{D}$ span the full spline space $\mathbb{F}_\mathcal{D}$.*

Proof. Theorem 2.12. of [16] implies that $\mathbb{P}_\mathcal{D} = \mathbb{F}_\mathcal{D}$. The result then follows immediately from Theorem 7 (ii). $\square$

Thus, we say that DPB-splines are *algebraically complete*.

5. Sufficient condition and examples

A hierarchy of patches π^ℓ and spaces $\mathbb{V}^\ell$, for $\ell = 1, \ldots, N$, will be called *feasible* if the corresponding patchwork spline space can be equipped with a DPB-spline basis. Therefore, in order to analyze whether a given hierarchy is feasible, we have to check if NNC, IPC

and SIC are satisfied for all patches and corresponding spline spaces. Verifying the latter two assumptions might be expensive since it requires us to go through all patch B-splines. However, for certain types of patches we can formulate conditions for IPC and SIC in the bivariate case, i.e., $d = 2$, that analyze only the boundary of a patch.

We define a *lower level boundary component* (LLBC) of a patch π^ℓ as a connected component of

$$\pi^k \cap \pi^\ell \neq \emptyset, \quad k < \ell.$$

Clearly, *IPC and SIC are satisfied for all patches with less than two LLBCs.*

In addition to this simple observation, we present a necessary and sufficient condition for a certain class of patches. A *fat* patch π^ℓ is the union of mutually disjoint boxes composed of at least $p_1 \times p_2$ cells in Z^ℓ, where vertically/horizontally adjacent boxes share a horizontal/vertical boundary segment of at least p_1/p_2 knot spans. We consider single LLBCs of π^ℓ and connected components of Γ^ℓ. These parts of the boundary are denoted as *critical boundary components* if they are enclosed by LLBC(s) at both ends.

Corollary 11. *IPC and SIC are satisfied for a fat patch π^ℓ if and only if the width or the height of each critical component δ equals at least p_1 or p_2 knot spans with respect to $\mathbb{V}^\ell$.*

Proof. First, we show that the condition on the critical components is sufficient. The intersection $\text{supp}\beta^\ell \cap \partial\pi^\ell$, for $\beta^\ell \in B^\ell$ is either empty, a horizontal or vertical line segment that is p_1 or p_2 knot spans long with respect to $\mathbb{V}^\ell$ or a polygon composed of a horizontal and vertical line segment with a maximum length of p_1 and p_2 knot spans, respectively. Therefore, if a patch B-spline β^ℓ intersects two LLBCs of π^ℓ, γ_1 and γ_2, then it holds that $\text{supp}\beta^\ell \cap \gamma_1 \cap \gamma_2 \neq \emptyset$. This implies IPC and SIC for π^ℓ.

Second, we prove that the condition is also necessary for IPC and SIC. We assume that there exists a critical boundary component δ that is joined to the LLBCs $\gamma_k \subseteq \pi^k$ and $\gamma_m \subseteq \pi^m$ at each end and does not meet the required assumption. Consequently, there exists a patch B-spline $\beta^\ell \in B^\ell$ such that

$$\text{supp}\beta^\ell \cap \gamma_k \neq \emptyset \ \text{ and } \ \text{supp}\beta^\ell \cap \gamma_m \neq \emptyset.$$

If $k = m$ then SIC is not fulfilled. For $k \neq m$ IPC can be only satisfied if there is another LLBC γ' of π^k or π^m such that $\text{supp}\beta^\ell \cap \gamma_m \cap \gamma' \neq \emptyset$ or $\text{supp}\beta^\ell \cap \gamma_k \cap \gamma' \neq \emptyset$, respectively. However, then SIC is violated either for level k or m. □

Example 3. We consider several examples of hierarchical meshes for spline spaces of degree $\mathbf{p} = (2, 2)$ and discuss if the hierarchies possess a DPB-spline basis, see Fig. 11. Note that IPC and SIC are automatically satisfied for a patch π^ℓ if it shares its boundary with higher level patches only, e.g., as it is the case for the first patch π^1. Furthermore, if there exists only one LLBC with respect to a level ℓ then IPC and SIC are satisfied for π^ℓ. Moreover, we analyze if we can construct a TPB-spline basis, see [40], or a THB-spline basis, see [14], on these meshes. A hierarchy is feasible for THB-splines if the spline spaces of all levels are nested. For TPB-splines the FSC and CBA assumption, see [40], have to be fulfilled in order to obtain a basis. Note that CBA is satisfied if all patches are aligned with the

knot lines of the corresponding spline space. We observe that the new construction of DPB-splines complements the other two bases.

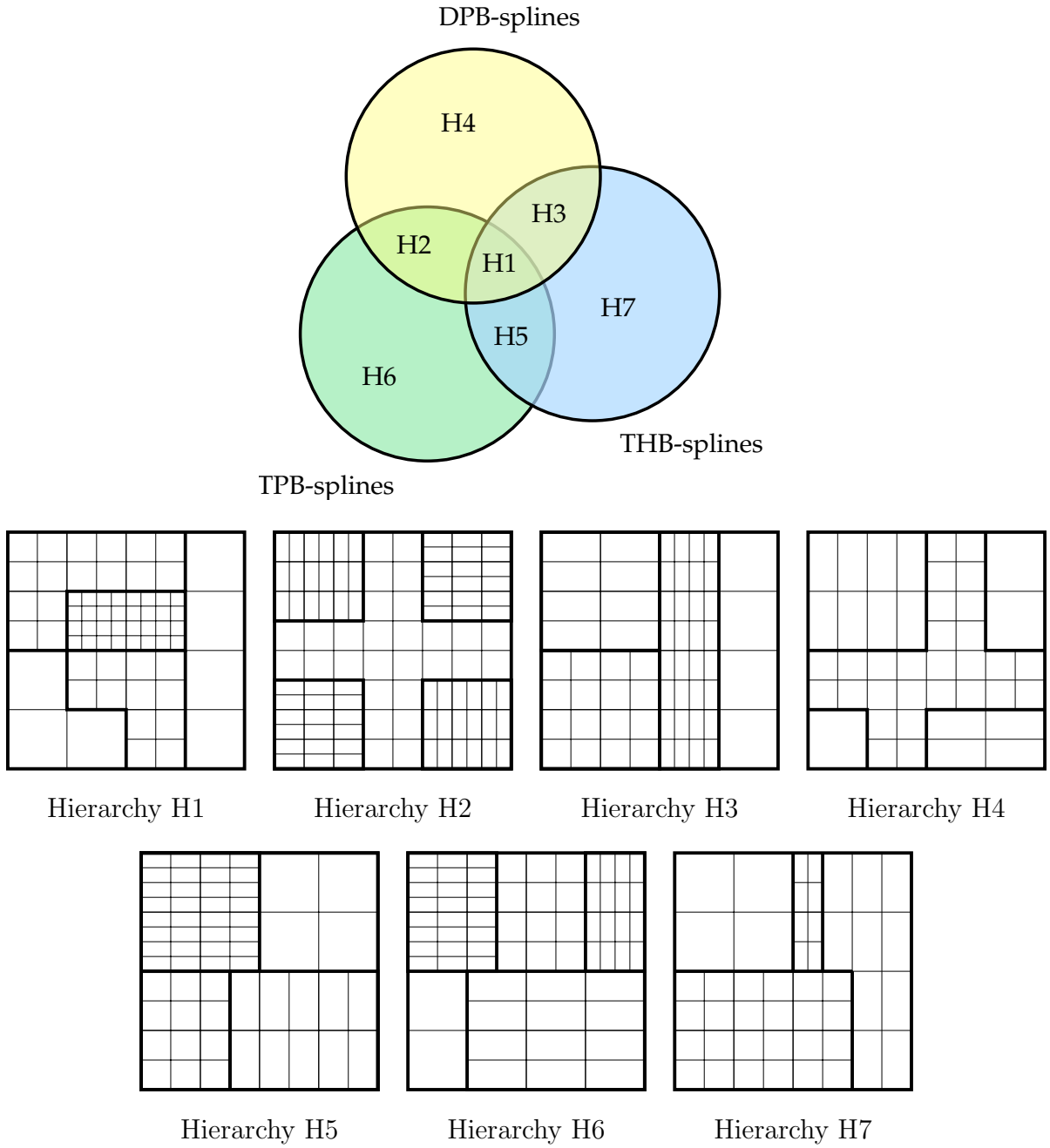

Figure 11: Venn diagram and hierarchical meshes for DPB-, TPB- and THB-splines.

Although there exist hierarchies that are valid for TPB- and not for DPB-splines we conjecture that this set is rather small compared to the set of hierarchies that possess a

DPB- and no TPB-spline basis. The following experimental example supports this assumption.

Example 4. We consider the regular subdivision of the unit square into 4×4 patches and randomly assign values from 0 to 3 to each patch. The spline spaces of the patches remain unchanged, are refined dyadically in x_1-direction, in x_2-direction and in both directions for the values 0, 1, 2 and 3, respectively. The patches are sorted according to these values, and patches with the same value are ordered randomly. We compute $120,000$ samples of such random hierarchies and analze how many of them are feasible for TPB- and DPB-splines. The results are reported in Table 1. Most of the samples ($114,605$) do not satisfy NNC and are unsuitable for all constructions. From the remaining $5,395$ hierarchies, 588 (approx. 11%) can be equipped with a DPB-spline basis, but only 4 (approx. 0.07%) admit a TPB-spline basis. 3 hierarchies are valid for TPB- and DPB-splines. The same experiment was performed for bicubic splines, on 3×3 patches with triadic refinement, see Table 1 last row. Finally, we note that very few (2 and 231) of the $120,000$ samples did not use anisotropic refinement, i.e., not the refinement values 1 and 2.

	nested	only DPB	only TPB	both
$\mathbf{p} = (2,2)$, 4×4 patches	$5,395$	588	4	3
$\mathbf{p} = (3,3)$, 3×3 patches	$25,169$	$11,636$	$2,011$	$1,757$

Table 1: Example 4 – Experimental quantification of patch structures suitable for TPB- and DPB-splines.

6. Iterative refinement

We consider bivariate tensor-product spline spaces of fixed degree $\mathbf{p} = (p_1, p_2)$ defined by uniform knot vectors obtained by performing r_i-times p_i-adic refinement in i–th direction, $i = 1, 2$. To be more precise, the spline space

$$\mathbb{S}^{\mathbf{r}} = \mathbb{S}^{(r_1, r_2)}$$

possesses the knot vector

$$(0, \dots, 0, \frac{1}{(p_i)^{r_i}}, \dots, \frac{(p_i)^{r_i} - 1}{(p_i)^{r_i}}, 1, \dots, 1),$$

in the i–th coordinate direction. These spline spaces are collected in a set, which we denote by $\mathfrak{S}$. A local spline space $\mathbb{V}^\ell$ is then defined as the restriction of a tensor-product spline space $\hat{\mathbb{V}}^\ell \in \mathfrak{S}$ to the corresponding patch. Consequently, there is a function

$$\mathbf{r} : \{1, \dots, N\} \to \mathbb{N} \times \mathbb{N}$$

such that $\hat{\mathbb{V}}^\ell = \mathbb{S}^{\mathbf{r}(\ell)}$ and

$$\mathbb{V}^\ell = \mathbb{S}^{\mathbf{r}(\ell)}|_{\pi^\ell}.$$

The knot lines of a spline space $\mathbb{S}^{\mathbf{r}}$ divide the domain into a set of cells $\hat{Z}^{\mathbf{r}}$. Hence, we obtain the local cell set

$$Z^\ell = \hat{Z}^{\mathbf{r}(\ell)}|_{\pi^\ell}.$$

We introduce a set of *macro elements* $\mathcal{M}^{\mathbf{r}}$, which contains the disjoint axis-aligned boxes consisting of $p_1 \times p_2$ cells in $\hat{Z}^{\mathbf{r}}$. To be more precise, the set $\mathcal{M}^{\mathbf{r}}$ contains the $p_1 \times p_2$ subgrids of $\hat{Z}^{\mathbf{r}}$ with lower left corners

$$(\frac{mp_1}{(p_1)^{r_1}}, \frac{np_2}{(p_2)^{r_2}}), \quad \text{for } m, n \in \mathbb{Z}.$$

We consider an iterative refinement procedure consisting of several *refinement steps*. The input is a hierarchy where the patches are equal to the macro elements of an initial tensor-product spline space $\mathbb{S}^{\mathbf{r}}$. In each refinement step we add knots to the spline spaces of certain marked patches, thereby generating patches with finer spline spaces. A *refinement indicator* marks the cells that should be refined and a *direction indicator* specifies the refinement direction, i.e., whether we perform knot insertion in the first (or u-) coordinate direction, second (or v-) coordinate direction, or both. We refine such that the tensor-product spline spaces of neighboring patches are nested. As a consequence the refinement is not according to the direction indicator in some cases. Furthermore, all cells of a marked patch will be refined to the same spline space. Hence, a marked patch is replaced by at least p_1, p_2 and $p_1 \times p_2$ patches, which are again macro elements, for refinement in u-, v- and both directions, respectively. After the knot insertion we sort the patches of the new hierarchy lexicographically with respect to $(r_1 + r_2, r_2)$. The ordering of the patches that belong to the same global spline space is chosen arbitrarily.

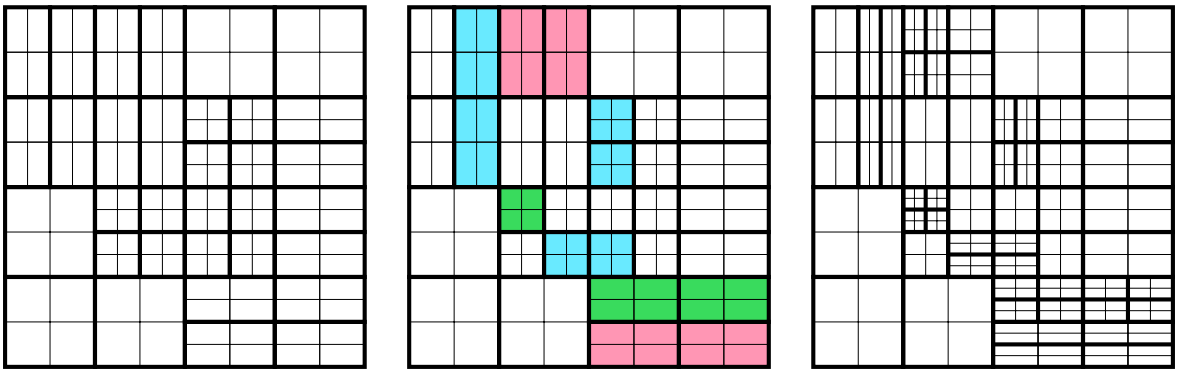

Figure 12: Example 5 – Illustration of one refinement step.

Example 5. We consider the hierarchy in Fig. 12 on the left for $\mathbf{p} = (2, 2)$. The first five patches are macro elements of the spline space $\mathbb{S}^{(3,3)}$, followed by eight macro elements from $\mathcal{M}^{(4,3)}$ and eight elements from $\mathcal{M}^{(3,4)}$. The last 12 patches are elements of

$\mathcal{M}^{(4,4)}$. The refinement and direction indicators mark certain patches for refinement as illustrated in the middle picture. Blue, red and green cells are marked for refinement in u-, v- and both directions, respectively. The image on the right shows the resulting mesh after the corresponding knot insertion. Note that the macro element with lower left corner $(\frac{1}{4}, \frac{3}{4})$ is marked for refinement in v-direction, which would result in non-nested spaces of neighboring patches. Therefore, we refine this patch in both directions instead. $\Diamond$

A hierarchy that is constructed by this refinement procedure is feasible for DPB-splines. NNC is satisfied. Moreover, all patches are boxes of size $p_1 \times p_2$ and according to the refinement mechanism, a patch shares an entire edge of its boundary either with a single patch of lower level or several patches of higher levels. Therefore, Corollary 11 guarantees that IPC and SIC are satisfied for all levels.

Furthermore, the so-constructed hierarchies also admit (T)PB-spline bases. Since all patches are aligned with the knot lines of the corresponding spline spaces CBA is satisfied. Moreover, the tensor-product basis functions $\hat{\beta}^\ell$ that do not vanish on the corresponding patch π^ℓ intersect only with neighboring patches of lower level or higher level patches where the corresponding spline space is a superspace of $\hat{\mathbb{V}}^\ell$. This implies that FSC is satisfied.

We use the refinement procedure in an iterative algorithm for approximating data with a DPB-spline surface by a standard regularized least-squares fitting, cf. [19]. The algorithm stops if the error does not exceed a user-defined threshold ε in a certain percentage of data points (usually between 95% and 99%) or the numbers of degrees of freedom or iteration steps exceed a predefined maximum.

One iteration of the *refinement algorithm* for least-squares fitting consists of the following steps:

- *Refinement indicator:* We mark all patches that contain points with an error exceeding a certain threshold.
- *Direction indicator:* The desired refinement direction for the marked elements is determined by a local-fitting method, see [40]. The direction indicator $\delta(\mu)$ takes the values 1, 2 or 3 for refinement in u-, v- and (u, v)-direction, respectively.
- *Determining a refinement order:* We sort the marked macro elements $\mu \in \mathcal{M}^{\mathbf{r}(\ell)}$, for $\ell = 1, \ldots, N$, lexicographically with respect to

$$(r_1(\ell) + r_2(\ell), r_2(\ell), \delta(\mu)).$$

  The elements are then refined one by one in this order.
- *Refinement of the elements:* The corresponding spline space of an element $\mu \in \mathcal{M}^{\mathbf{r}(\ell)}$ is refined to a new spline space $\mathbb{V}^{\mathbf{r}(k)}$ that satisfies

  (i) $r_i(k) \geq r_i(\ell)$, for $i = 1, 2$,

  (ii) $\mathbb{S}^{\mathbf{r}(k)}$ is nested with the current spline spaces of neighboring patches, and

	no. of dof	% of dof	max. error	avg. error	overall time
SPR – 1 patch	$13,579$	100%	$6.9e{-4}$	$2.24e{-5}$	8min 34sec
SPR – 4 patches	$21,607$	159%	$1e{-3}$	$2.28e{-5}$	1h 8min
MER – $(2,2)$	$9,732$	71.7%	$6.4e{-4}$	$2.44e{-5}$	5min 46sec
MER – $(3,3)$	$9,732$	71.7%	$6.4e{-4}$	$2.44e{-5}$	5min 40sec
MER – $(4,4)$	$9,732$	71.7%	$6.4e{-4}$	$2.44e{-5}$	4min 52sec

Table 2: Table for Example 6

(iii) $|r_1(k) - r_2(k)| \leq 3$.

Note that the property (iii) controls the aspect ratio of the elements. If refinement according to the direction indicator does not result in a space that fulfills these properties then we choose the smallest $\mathbf{r}(k)$ with respect to the lexicographical ordering $(r_1 + r_2, r_2)$ that satisfies them.

- *Final ordering:* We sort all macro elements lexicographically with respect to $(r_1 + r_2, r_2)$ and apply the selection mechanism.

Example 6. We approximate the data set of Example 6 in [40] by biquadratic splines, i.e., $\mathbf{p} = (2,2)$, and compare the hierarchies obtained from the macro element refinement (MER) and the original, simple patch refinement (SPR) algorithm presented in [40].

For both algorithms we choose the initial spline space $\mathbb{S}^{(3,3)}$, thus we obtain 4×4 initial macro elements/patches for MER. For SPR, the initial number of patches is user-defined and we decide to start from a single patch. The regularized least-squares fitting is solved with smoothness parameter $\lambda = 1d - 7$ and the iteration stops if the error in $\geq 98\%$ of the points is lower or equal to the threshold $\varepsilon = 1e - 4$. Fig. 13 depicts the resulting surface and meshes of both algorithms. Table 2 presents the number of degrees of freedom, some error statistics and computation times for both methods in rows 1 and 4, respectively. We observe that MER achieves a similar good result with fewer degrees of freedom than SPR. Furthermore, the sorting and possible additional refinement that is necessary for generating a feasible hierarchy in SPR is not required by MER, which is reflected in the lower computational times. The more patches are present in a hierarchy the more pronounced difference becomes.

Moreover, we observed that SPR is very sensitive to the choice of the initial setting. If we choose the same initial spline space but start from four patches we obtain significantly worse results, see Table 2, second row. Therefore, in order to obtain good results in terms of number of degrees of freedom and computation time it is crucial to find a suitable initial setting for SPR. In contrast to this, the initial setting for MER is defined by the initial spline space only. We obtained nearly equivalent results for sufficiently coarse initial layouts, see row 3 and 5 of Table 2. $\Diamond$

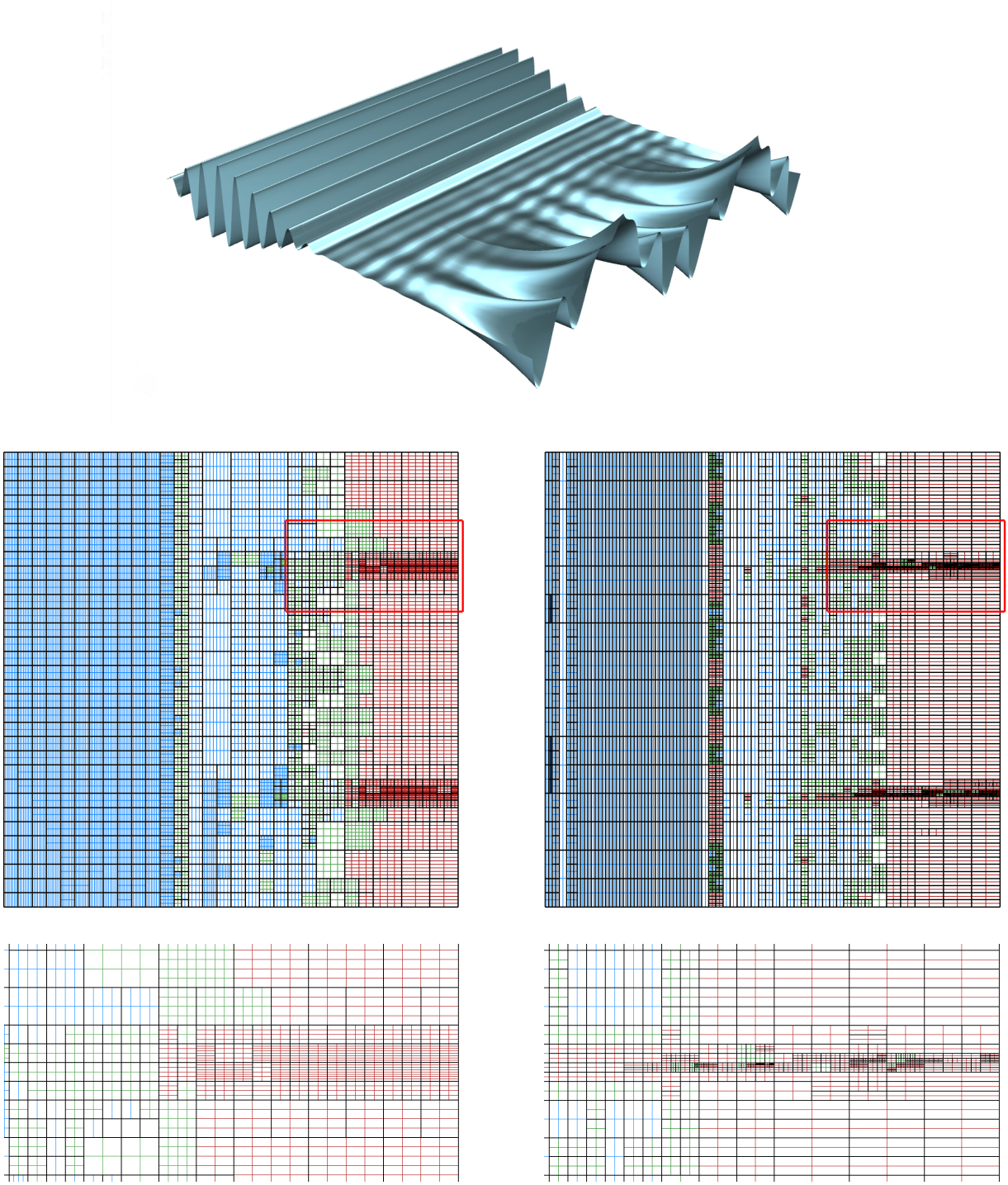

Figure 13: Example 6 – Approximated surface (top) and corresponding meshes for SPR (left) and MER (right). Patch boundaries are black. The knot lines of a spline space $\mathbb{S}^{(r_1,r_2)}$ are colored according to the dominant refinement direction, from blue ($r_1 > r_2$) via green ($r_1 = r_2$) to red ($r_1 < r_2$).

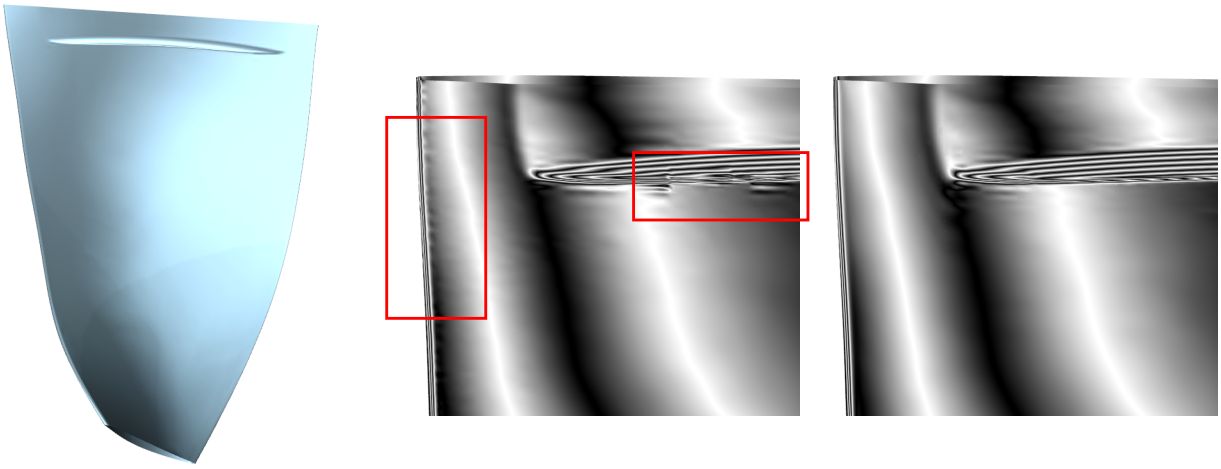

Figure 14: Example 7 – Approximated surface (left) and reflection line analysis for SPR (middle) and MER (right).

Example 7. We reconstruct a real-world aircraft engine blade from $\approx 300,000$ data points, which were obtained by optical scanning. Many industrial applications require C^2-smooth surfaces and thus, the data set is approximated by bicubic splines. We set $\lambda = 5d - 7$, $\varepsilon = 2d - 5$ and stop the iteration if $\geq 95\%$ of the data points are below the threshold. Again we compare the results of the SPR and MER algorithm, see Fig. 14 and 15 for images of the geometry and the meshes and Table 3 for statistics.

The SPR algorithm uses dyadic knot refinement and starts from the initial hierarchy consisting of 8 patches with initial spline spaces defined by the periodic knot vectors

$$(-\frac{3}{32}, -\frac{2}{32}, -\frac{1}{32},\ 0\ , \frac{1}{32}, \ldots, \frac{31}{32},\ 1\ , \frac{33}{32}, \frac{34}{32}, \frac{35}{32})$$

in both directions. The resulting mesh from the iterative fitting process is depicted in Fig. 15 (left) and additional information is given in the first row of Table 3. Changing the initial setting for SPR again leads to a drastically different result, see row 2 of Table 3.

For MER we start from the initial spline space $\mathbb{S}^{(3,3)}$ with periodic knot vectors and perform triadic knot refinement. The resulting mesh is depicted in Fig. 15 on the right. As before, the algorithm yields a result with fewer degrees of freedom and less computation time but comparable errors, see fourth row of Table 3. Furthermore, MER leads to a surface with a better visual quality compared to the result obtained by SPR, see Fig. 14. The SPR based surface (center) possesses oscillations that are not present or less pronounced in the MER based surface (right). Choosing the initial spline spaces $\mathbb{S}^{(2,2)}$ and $\mathbb{S}^{(4,4)}$ again leads to similar results, see rows 3 and 5 of Table 3. Although the numbers of degrees of freedom vary, all three initial settings need similar computation time and lead to similar approximation errors. $\Diamond$

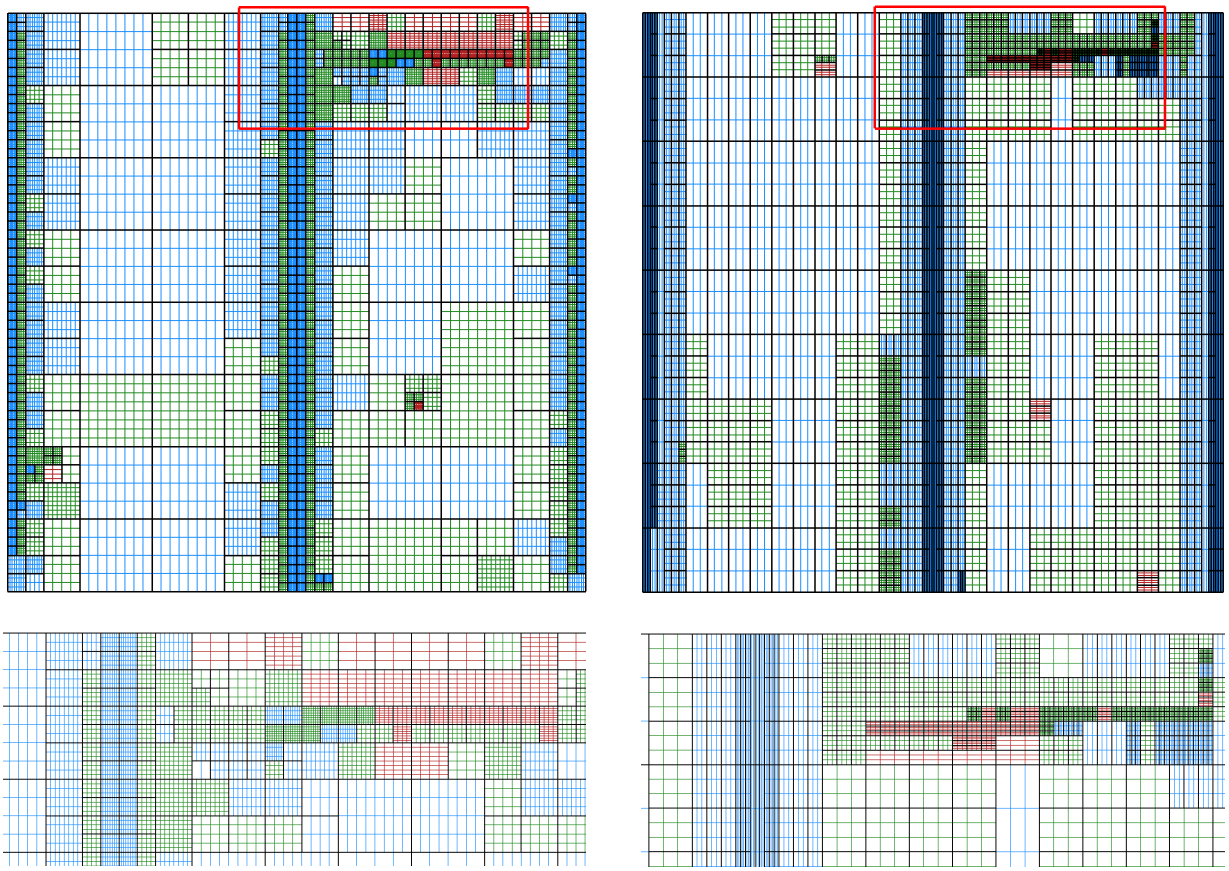

Figure 15: Example 7 – Meshes for SPR (left) and MER (right).

	no. of dof	% of dof	max. error	avg. error	overall time
SPR – 16 patches	$19,823$	100%	$5.0e{-5}$	$3.32e{-6}$	17min 38sec
SPR – 64 patches	$31,184$	157.3%	$1.1e{-3}$	$3.51e{-6}$	54min 40sec
MER – $(2,2)$	$9,774$	49.3%	$5.6e{-5}$	$3.84e{-6}$	11min 47sec
MER – $(3,3)$	$13,284$	67%	$5.6e{-5}$	$3.33e{-6}$	10min 20sec
MER – $(4,4)$	$24,498$	123.6%	$5.6e{-5}$	$3.01e{-6}$	14min

Table 3: Table for Example 7

7. Conclusion

The definition of a TPB-spline basis requires a strong nestedness assumption, which limits the choice of possible refinement strategies. The new construction of DPB-splines, which was presented in this paper, substantially increases the flexibility for anisotropic refinement. The use of locally defined, decoupled basis functions enables the definition of a basis under three assumptions (NNC, IPC and SIC) that affect only the direct neighborhood of a patch. In particular, only the spaces associated with neighboring patches have to be nested. Furthermore, for a certain class of patches we identified a particularly simple sufficient condition for IPC and SIC.

The DPB-splines possess the required order of smoothness, they span the patchwork spline space, form a non-negative partition of unity and preserve the coefficients of the local B-spline representations. Moreover, the DPB-splines are algebraically complete, i.e., the patchwork spline space is equal to the full spline space. This property is not necessarily satisfied for the (T)PB-splines. Although there exist some hierarchies that are valid for TPB-splines but cannot be equipped with a DPB-spline basis, this set is rather small compared to the hierarchies that are feasible for DPB-splines and do not allow the definition of a TPB-spline basis.

Finally, the definition of DPB-splines inspired us to introduce a new refinement algorithm for least-squares fitting. The resulting hierarchies admit a PB-, TPB- and DPB-spline basis. Furthermore, this macro element-based refinement offers the significant advantage that a feasible hierarchy is automatically generated without the additional sorting and refinement that is required for the previous SPR algorithm presented in [40]. This enabled us to reduce the computation time and the number of degrees of freeedom compared to SPR, while preserving the high quality of the results.

Acknowledgment. Supported by the Austrian Science Fund (FWF) through project NFN S117 "Geometry + Simulation" and by the European Research Council (ERC) through the grant "CHANGE" (GA no. 694515).

References

[1] D. Mokriš, B. Jüttler, TDHB-splines: The truncated decoupled basis of hierarchical tensor-product splines, Comput. Aided Geom. Design 31 (7–8) (2014) 531–544.

[2] G. Farin, J. Hoschek, M.-S. Kim (Eds.), Handbook of Computer Aided Geometric Design, Elsevier, 2002.

[3] D. R. Forsey, R. H. Bartels, Hierarchical B-spline refinement, Comput. Graphics 22 (1988) 205–212.

[4] R. Kraft, Adaptive und linear unabhängige Multilevel B-splines und ihre Anwendungen, Ph.D. thesis, Univ. Stuttgart (1998).

[5] T. W. Sederberg, J. Zheng, A. Bakenov, A. Nasri, T-splines and T-NURCCS, ACM Trans. Graphics 22 (2003) 477–484.

[6] X. Li, J. Zheng, T. W. Sederberg, T. J. R. Hughes, M. A. Scott, On linear independence of T-spline blending functions, Comput. Aided Geom. Design 29 (2012) 63–76.

[7] L. B. da Veiga, A. Buffa, D. Cho, G. Sangalli, Analysis-suitable T-splines are dual-compatible, Comput. Meth. Appl. Mech. Engrg. 249–252 (2012) 42–51.

[8] P. Morgenstern, D. Peterseim, Analysis-suitable adaptive T-mesh refinement with linear complexity, Comput. Aided Geom. Design 34 (2015) 50–66.

[9] J. Zhang, X. Li, Local refinement for analysis-suitable++ T-splines, Comput. Meth. Appl. Mech. Engrg. 342 (2018) 32–45.

[10] X. Li, J. Deng, F. Chen, Polynomial splines over general T-meshes, Visual Comput. 26 (2010) 277–286.

[11] H. Kang, J. Xu, F. Chen, J. Deng, A new basis for PHT-splines, Graphical Models 82 (2015) 149–159.

[12] T. Dokken, T. Lyche, K. F. Pettersen, Polynomial splines over locally refined box-partitions, Comput. Aided Geom. Design 30 (2013) 331–356.

[13] L. Chen, R. de Borst, Locally refined T-splines, Int. J. Numer. Meth. in Engrg. 114 (6) (2018) 637–659.

[14] C. Giannelli, B. Jüttler, H. Speleers, THB-splines: The truncated basis for hierarchical splines, Comput. Aided Geom. Design 29 (2012) 485–498.

[15] C. Giannelli, B. Jüttler, H. Speleers, Strongly stable bases for adaptively refined multilevel spline spaces, Adv. Comput. Math. 40 (2) (2014) 459–490.

[16] D. Mokriš, B. Jüttler, C. Giannelli, On the completeness of hierarchical tensor-product B-splines, J. Comput. Appl. Math. 271 (2014) 53–70.

[17] H. Speleers, C. Manni, Effortless quasi-interpolation in hierarchical spaces, Numerische Mathematik 132 (1) (2016) 155–184.

[18] G. Greiner, K. Hormann, Interpolating and approximating scattered 3D-data with hierarchical tensor product B-splines, in: A. L. Méhauté, C. Rabut, L. Schumaker (Eds.), Surface Fitting and Multiresolution Methods, Vanderbilt University Press, Nashville, TN, 1997, pp. 163–172.

[19] G. Kiss, C. Giannelli, U. Zore, B. Jüttler, D. Großmann, J. Barner, Adaptive CAD model (re-)construction with THB-splines, Graph. Models 76 (5) (2014) 273–288.

[20] C. Bracco, C. Giannelli, D. Großmann, A. Sestini, Adaptive fitting with THB-splines: Error analysis and industrial applications, Comput. Aided Geom. Design 62 (2018) 239 – 252.

[21] P. B. Bornemann, F. Cirak, A subdivision-based implementation of the hierarchical B-spline finite element method, Comput. Meth. Appl. Mech. Engrg. 253 (2013) 584–598.

[22] A. Buffa, C. Giannelli, Adaptive isogeometric methods with hierarchical splines: error estimator and convergence, Math. Meth. Appl. Sc. 26 (2016) 1–25.

[23] G. Kuru, C. Verhoosel, K. van der Zeeb, E. Brummelen, Goal-adaptive isogeometric analysis with hierarchical splines, Comput. Meth. Appl. Mech. Engrg. 270 (2014) 270–292.

[24] D. Schillinger, et al., An isogeometric design-through-analysis methodology based on adaptive hierarchical refinement of NURBS, immersed boundary methods, and T-spline CAD surfaces, Comput. Meth. Appl. Mech. Engrg. 249–252 (2012) 116–150.

[25] H. Atri, S. Shojaee, Truncated hierarchical B-splines in isogeometric analysis of thin shell structures, Steel and Composite Structures 26 (2) (2018) 171–182.

[26] C. Bracco, A. Buffa, C. Giannelli, R. Vázquez, Adaptive isogeometric methods with hierarchical splines: An overview, Discrete and Continuous Dynamical Systems- Series A 39 (1) (2019) 241–262.

[27] C. Giannelli, et al., THB-splines: An effective mathematical technology for adaptive refinement in geometric design and isogeometric analysis, Comput. Meth. Appl. Mech. Engrg. 299 (2016) 337–365.

[28] E. Garau, R. Vázquez, Algorithms for the implementation of adaptive isogeometric methods using hierarchical B-splines, Applied Numerical Mathematics 123 (2018) 58–87.

[29] H. Speleers, P. Dierckx, S. Vandewalle, Quasi-hierarchical Powell-Sabin B-splines, Comput. Aided Geom. Design 26 (2009) 174–191.

[30] A. Yvart, S. Hahmann, G.-P. Bonneau, Hierarchical triangular splines, ACM Trans. Graphics 24 (2005) 1374–1391.

[31] T. Kanduč, C. Giannelli, F. Pelosi, H. Speleers, Adaptive isogeometric analysis with hierarchical box splines, Comput. Meth. Appl. Mech. Engrg. 316 (2017) 817–838.

[32] U. Zore, B. Jüttler, Adaptively refined multilevel spline spaces from generating systems, Comput. Aided Geom. Design 31 (2014) 545–566.

[33] C. Giannelli, T. Kanduč, F. Pelosi, H. Speleers, An immersed-isogeometric model: Application to linear elasticity and implementation with THBox-splines, J. Comput. Appl. Math. 349 (2019) 410–423.

[34] H. Kang, F. Chen, J. Deng, Hierarchical B-splines on regular triangular partitions, Graph. Models 76 (5) (2014) 289–300.

[35] E. J. Evans, M. A. Scott, X. Li, D. C. Thomas, Hierarchical T-splines: analysis-suitability, Bézier extraction, and application as an adaptive basis for isogeometric analysis, Comput. Meth. Appl. Mech. Engrg. 284 (2015) 1–20.

[36] L. Chen, R. de Borst, Adaptive refinement of hierarchical T-splines, Comput. Meth. Appl. Mech. Engrg. 337 (2018) 220–245.

[37] X. Wei, Y. Zhang, T. J. R. Hughes, M. A. Scott, Extended truncated hierarchical Catmull-Clark subdivision, Comput. Meth. Appl. Mech. Engrg. 299 (2016) 316–336.

[38] U. Zore, B. Jüttler, J. Kosinka, On the linear independence of truncated hierarchical generating systems, J. Comput. Appl. Math. 306 (2016) 200–216.

[39] N. Engleitner, B. Jüttler, U. Zore, Partially nested hierarchical refinement of bivariate tensor-product splines with highest order smoothness, in: M. Floater, et al. (Eds.), Mathematical Methods for Curves and Surfaces, Lecture Notes in Computer Science, Springer, 2017, pp. 126–144.

[40] N. Engleitner, B. Jüttler, Patchwork B-spline refinement, Comput. Aided Design 90 (2017) 168–179.

[41] N. Engleitner, B. Jüttler, Lofting with Patchwork B-splines, in: Springer INdAM Series, Springer, 2019, *in press*.